DOI:
10.1287/mnsc.2016.2488

Tail Risk Dynamics in Stock Returns: Links to the Macroeconomy and Global Markets Connectedness*

Daniele Massacci

Bank of England

February 20, 2016

Abstract

We propose a new time-varying peaks over threshold model to study tail risk dynamics in equity markets: the laws of motion for the parameters are defined through the score-based approach. We apply the model to daily returns from U.S. size-sorted decile stock portfolios and show that large firms tail risk increases during recessions more than small firms tail risk. Our results are consistent with the granular hypothesis of aggregate fluctuations and we quantify the impact of large firms tail risk shocks on the economy. A measure of tail connectedness is proposed: evidence from international equity markets shows that tail connectedness increases during periods of turmoil.

JEL classification: C22, E32, G10, G15.

Keywords: Time-Varying Tail Risk, Score-Based Model, Stock Returns, Uncertainty, Tail Connectedness.

*This work was carried out when I was Franco Modigliani Research Fellow in Economics and Finance at EIEF; it was not carried out at the Bank of England. The views in this paper are mine and do not reflect those of the Bank of England. I am indebted to Andrew Harvey for several invaluable suggestions. I thank Davide Delle Monache and Ivan Petrella for introducing me to score-based models; and Hashem Pesaran for hosting me at CAFE, USC, and for providing me with some of the data. I am grateful to Simone Emiliozzi, Domenico Giannone, Luigi Guiso, Marco Lippi, Dale Rosenthal, Emiliano Santoro, Lucio Sarno, David Veredas, Xin Zhang and participants to the "Skewness, Heavy Tails, Market Crashes and Dynamics" conference in Cambridge, the EIEF lunch seminar and the "Sixth Italian Congress of Econometrics and Empirical Economics (ICEEE-6th)" in Salerno for helpful comments and suggestions. I thank three referees, an associate editor, and the department editor (Lauren Cohen) for the insightful comments. Errors and omissions are my own responsibility. Financial support from Associazione Borsisti Marco Fanno and UniCredit & University Foundation is gratefully acknowledged.

1 Introduction

Financial risk measurement is central for portfolio risk minimization and for monitoring stability in financial markets. A voluminous literature provides econometric tools to measure risk during tranquil times (see Andersen *et al.* (2013) and references therein). Financial returns are conditionally fat-tailed (Bollerslev (1987)) and risk measures valid during tranquil periods may not be informative in turbulent times: these are periods when large positive or negative realizations of financial returns are more likely to occur and it becomes important to estimate the probability of these extreme returns. This leads to the concept of *tail risk*: measuring tail risk can be difficult in practice since the conditional distribution of financial returns during periods of distress may not be appropriately described under standard parametric assumptions. This paper provides a threefold contribution to the literature on tail risk measurement in financial markets: it develops a novel econometric model to quantify tail risk; it studies the links to the macroeconomy; and it proposes a measure of tail connectedness across different markets.

A powerful tool to measure tail risk is extreme value theory (EVT) (Embrechts *et al.* (1997)), which approximates the distribution of random variables along the lower and upper tails. EVT has been used in empirical finance to measure tail risk from the unconditional distribution of returns. Koedijk *et al.* (1990) and Hols and de Vries (1991) apply the power law to exchange rate returns, while Jansen and de Vries (1991) focus on the stock market. Akgiray and Booth (1988), Longin and Solnik (2001) and Poon *et al.* (2004) employ the peaks over threshold (POT) of Picklands (1975) and Davison and Smith (1990) to model the distribution of extreme returns in equity markets: the building block of the POT is the generalized Pareto distribution (GPD).

Estimation of the tails of the unconditional distribution of returns is informative under the maintained assumption of random sampling: the data generating processes of financial returns however exhibit structural breaks and time-varying dynamics such as volatility clustering, which create non-stationarities that lead to model misspecification if neglected (Kearns and Pagan

(1997), Diebold *et al.* (1998) and Chavez-Demoulin and Davison (2012)). Quintos *et al.* (2001) build formal tests to detect structural breaks, which Werner and Upper (2002) and Galbraith and Zernov (2004) use to analyze Bund futures returns and U.S. equity returns, respectively.

There exist two strategies to account for non-stationarities when modelling extremes (Chavez-Demoulin and Davison (2012)). The first uses the original data to parameterize and estimate non-stationarities, and then fits EVT models for stationary series to the resulting residuals. McNeil and Frey (2000) apply a time-varying volatility model to financial returns and then use the static POT: volatility models assume that extreme returns have the same conditional distribution as the rest of the returns and model misspecification may persist (Engle and Manganelli (2004)). The second strategy fits an EVT model robust to non-stationarities to the original data. Chavez-Demoulin *et al.* (2014) use Bayesian methods to build a nonparametric POT model with regime switches driven by a Poisson process. Allen *et al.* (2012), Kelly (2014) and Kelly and Jiang (2014) propose an alternative and very interesting route: they build dynamic measures of tail risk by devising panel approaches that exploit both the time series and the cross-sectional dimensions of the available data.

We opt for the second strategy and propose a novel EVT model robust to non-stationarities. As in Chavez-Demoulin *et al.* (2014), this paper relies on pure time series methods and builds a dynamic POT model. Rather than working with Bayesian statistics, we model the time-varying parameters using the frequentist approach. Cox (1981) distinguishes between two classes of models with dynamic parameters: observation-driven and parameter-driven models. In the former, the laws of motion for the parameters are in terms of functions of observable variables: popular examples are the ARCH model by Engle (1982), the GARCH by Bollerslev (1986, 1987), the autoregressive conditional density by Hansen (1994), and the recent score-based autoregressive models by Creal *et al.* (2012) and Harvey (2013). In parameter-driven models, the parameters are stochastic processes with an error component: examples are stochastic volatility models (Shephard (2005)). Wagner (2005) combines the power law and the parameter-driven approach to dynamically estimate the tail index. We follow the observation-driven approach and apply the data-driven score-based principle of Creal *et al.* (2012) and Harvey (2013): the result is an unobserved components model (Harvey (1989, 2013)); and observation-driven unobserved component models have successfully studied the links between the conditional distribution of asset returns and the macroeconomic environment (see Engle *et al.* (2013) and references therein). To the best of our knowledge, this approach is new to the literature on tail risk measurement: it is the first, as well as the methodological contribution of the paper. Our model improves also with respect to the quantile regression framework of Engle and Manganelli (2004): the observable innovation for the time-varying quantiles is *a priori* specified and not data-driven.

We apply the model to uncover the links between tail risk and the macroeconomy: this second contribution places our work within a growing literature (Allen *et al.* (2012), Kelly (2014), Kelly and Jiang (2014), and Giglio *et al.* (2015)), and it complements studies on the linkages between volatility and the macroeconomy (see Andersen *et al.* (2013) and Engle *et al.* (2013) and the references therein). Using returns on U.S. decile-sorted equity portfolios, we show that tail risk is countercyclical and that its correlation with the business cycle increases in firm size: large firms uncertainty then is more sensitive to the business cycle than small firms uncertainty. To the very best of our knowledge, this provides an original contribution to the literature on micro uncertainty, which has shown that firm-level uncertainty is countercyclical (Bloom (2014) and Bloom *et al.* (2014)): we make one further step and document that the dynamics of firm-level uncertainty over the business cycle depend on firm size. Using an identification strategy based on the time series, we show that our findings are consistent with Gabaix (2011) granular hypothesis of fluctuations: the distribution of firms is highly fat-tailed, the central limit theorem does not apply and idiosyncratic shocks to large firms drive aggregate fluctuations. We quantify the effects of large firms tail risk shocks on the economy: this contributes to the empirical literature on measuring the effects of uncertainty shocks (Bloom (2009), Kelly and Jiang (2014) and Jurado *et al.* (2015)) by taking into account Gabaix (2011) granular hypothesis.

Finally, we build a measure of connectedness amongst the tails of the conditional distribution of returns: to the very best of our knowledge, this is new to the literature and provides an additional measure of risk. Our work relates to studies that look at risk concentration along the cross-sectional dimension using either returns or volatilities as risk drivers (Billio *et al.* (2012) and Diebold and Yilmaz (2014)). We monitor global equity markets and show that tail connectedness increases during periods of turmoil: this resembles the results in Diebold and Yilmaz (2009) with respect to volatility connectedness and suggests that diversification over international markets may not hedge against tail risk. Tail connectedness cannot be measured using the panel approach of Allen *et al.* (2012), Kelly (2014) and Kelly and Jiang (2014), as this exploits the entire cross-section of returns to estimate tail risk.

2 Modelling the Conditional Distribution of Extreme Returns

2.1 Conditional Distribution of Extreme Returns

Let $\{R_t\}_{t=1}^{T}$ be the time sequence of random returns on a portfolio of risky assets, where T denotes the size of the available sample. Following common practice in the literature, extreme returns are defined in terms of exceedances with respect to a fixed threshold value γ (Chavez-Demoulin *et al.* (2014)): we refer to the events $R_t < \gamma$ and $R_t > \gamma$ as to negative and positive exceedances, respectively. The choice of γ is important and it is carefully discussed in Section 2.3.1 below. For expositional purposes, we focus on positive exceedances: analogous results hold for negative exceedances by an argument of symmetry. Let $F_t\left(r_t\left|\mathfrak{F}_{t-1}\right.\right)$ be the conditional cumulative distribution function of R_t, where $\mathfrak{F}_t$ denotes the information set available at period t: we let $F_t\left(r_t\left|\mathfrak{F}_{t-1}\right.\right)$ generally be time-varying; we also assume it is absolutely continuous and positive everywhere on the real line for all t, so that an underlying probability density function for R_t exists at each point in time. For a given quantile q_t of the conditional distribution of R_t, it follows that $\Pr\left(R_t \leq q_t\left|\mathfrak{F}_{t-1}\right.\right) = F_t\left(q_t\left|\mathfrak{F}_{t-1}\right.\right)$; the event $R_t > \gamma$ is then assigned a conditional probability $p_t = \Pr(R_t > \gamma \,|\mathfrak{F}_{t-1}) = 1 - F_t(\gamma\,|\mathfrak{F}_{t-1})$. Since we focus on positive exceedances, we work under the maintained assumption $\gamma > 0$.

Let the conditional cumulative distribution function of positive exceedances over γ be

$$F_t^{\gamma}(r_t\,|\mathfrak{F}_{t-1}) = \Pr(\gamma < R_t \leq r_t\,|R_t > \gamma; \mathfrak{F}_{t-1}) = \frac{F_t(r_t\,|\mathfrak{F}_{t-1}) - F_t(\gamma\,|\mathfrak{F}_{t-1})}{1 - F_t(\gamma\,|\mathfrak{F}_{t-1})}, \quad 0 < \gamma \leq r_t,$$

which is unknown without distributional assumptions on the sequence of returns $\{R_t\}_{t=1}^{T}$, namely without assumptions about the analytical expression for $F_t(r_t\,|\mathfrak{F}_{t-1})$. An approximation for $F_t^{\gamma}(r_t\,|\mathfrak{F}_{t-1})$ is available under the POT of Picklands (1975) and Davison and Smith (1990): following Balkema and De Haan (1974) and Picklands (1975), the GPD is the only non-degenerate distribution that approximates that of exceedances as the threshold γ approaches the upper bound of the conditional distribution of R_t. As in Harvey (2013), we write the conditional cumulative distribution function of the GPD for $R_t > \gamma$ as[1]

$$G_t^{\gamma}(r_t\,|\mathfrak{F}_{t-1}) = 1 - \left(1 + \frac{r_t - \gamma}{\alpha_t}\right)^{-\varsigma_t}, \quad r_t > \gamma, \quad \gamma > 0, \quad \varsigma_t > 0, \quad \alpha_t > 0: \tag{1}$$

both the shape parameter ς_t and the scale parameter α_t are time-varying, so that $G_t^{\gamma}(r_t\,|\mathfrak{F}_{t-1})$ is time-dependent. The following uniform convergence result as applied to $F_t^{\gamma}(r_t\,|\mathfrak{F}_{t-1})$ holds (Balkema and De Haan (1974) and Picklands (1975)):

$$\lim_{\gamma \to +\infty} \sup_{\gamma \leq r_t < +\infty} \left|F_t^{\gamma}(r_t\,|\mathfrak{F}_{t-1}) - G_t^{\gamma}(r_t\,|\mathfrak{F}_{t-1})\right| = 0. \tag{2}$$

The shape of $G_t^{\gamma}(r_t\,|\mathfrak{F}_{t-1})$ depends on ς_t and α_t (see Smith (1985), Davison and Smith (1990) and Ledford and Tawn (1996) for technical details). The scale parameter $\alpha_t > 0$ depends on the threshold γ. The parameter ς_t is independent of γ and determines the shape of the upper tail of the conditional distribution of returns: the assumption $\varsigma_t > 0$ follows from the fact that the

[1] See Harvey (2013), Section 5.3.5.

distribution of returns is heavy-tailed and obeys the power law (e.g., student-t distribution as in Bollerslev (1987)). The limiting case $\varsigma_t \to \infty$ leads to an exponentially declining tail and the function $p_t = \Pr(R_t > \gamma \,|\mathfrak{F}_{t-1})$ monotonically decreases in ς_t: lower values for ς_t are associated to higher tail risk. We refer to ς_t as to the shape parameter or the tail index. The aim is to characterize the dynamic properties of ς_t, a sufficient statistic for tail risk.

The conditional cumulative distribution function of the GPD in (1) applies only to realizations of R_t above γ. We wish to have a sequence $\{\varsigma_t\}_{t=1}^{T}$ for all t to measure tail risk over the entire sample space of R_t. Since the POT is only informative about the distribution of R_t above γ, we treat realizations of R_t below γ as censored at γ (Davison and Smith (1990), Ledford and Tawn (1996) and Longin and Solnik (2001)). Define $Y_t = \max(R_t - \gamma, 0)$, with corresponding conditional cumulative distribution function $\Pr(Y_t \leq y_t \,|\mathfrak{F}_{t-1}) = H_t(y_t \,|\mathfrak{F}_{t-1})$: for $y_t = 0$ it follows that $H_t(y_t \,|\mathfrak{F}_{t-1}) = 1 - p_t$; and from (1), for $y_t > 0$ we obtain the approximation

$$H_t(y_t \,|\mathfrak{F}_{t-1}) = 1 - p_t + p_t G_t^{\gamma}(r_t \,|\mathfrak{F}_{t-1}) = 1 - p_t\left(1 + \frac{y_t}{\alpha_t}\right)^{-\varsigma_t}, \quad y_t > 0, \quad \varsigma_t > 0, \quad \alpha_t > 0.$$

Let $\mathbb{I}(\cdot)$ denote the indicator function; the conditional distribution function of Y_t then is

$$H_t(y_t \,|\mathfrak{F}_{t-1}) = \mathbb{I}(y_t = 0)(1 - p_t) + \mathbb{I}(y_t > 0)\left[1 - p_t\left(1 + \frac{y_t}{\alpha_t}\right)^{-\varsigma_t}\right], \quad \varsigma_t > 0, \quad \alpha_t > 0: \qquad (3)$$

a realization $y_t > 0$ tells the model that the exceedance is drawn from the continuous GPD; when $y_t = 0$ we only know that the return does not belong to the tail.

The function $H_t(y_t \,|\mathfrak{F}_{t-1})$ in (3) requires information about $p_t = \Pr(R_t > \gamma \,|\mathfrak{F}_{t-1})$. The heavy-tailed conditional distribution of returns belongs to the maximum domain of attraction of the Fréchet distribution (see Embrechts *et al.* (1997)): we then approximate p_t as a power law multiplied by a time-varying function $L_t(q_t)$ slowly varying at infinity. Formally,

$$\Pr(R_t > q_t \,|\mathfrak{F}_{t-1}) = L_t(q_t)\, q_t^{-\varsigma_t}, \quad \lim_{q_t \to +\infty} \frac{L_t(cq_t)}{L_t(q_t)} = 1, \quad q_t > 0, \quad \varsigma_t > 0, \quad c > 0. \qquad (4)$$

We parameterize the function $L_t(q_t)$ as

$$L_t(q_t) = \left(\frac{q_t}{1+q_t}\right)^{\varsigma_t}, \quad q_t > 0, \quad \varsigma_t > 0. \tag{5}$$

From (4) and (5) it follows that

$$p_t = \Pr(R_t > \gamma \,|\mathfrak{F}_{t-1}) = \left(\frac{1}{1+\gamma}\right)^{\varsigma_t}, \quad \gamma > 0, \quad \varsigma_t > 0: \tag{6}$$

the parameterization of $L_t(q_t)$ in (5) ensures that p_t in (6) lies within the unit interval and it is a probability measure for all $\gamma > 0$; p_t is monotonically decreasing in γ and ς_t, and it satisfies $\lim_{\gamma\to 0} p_t = 1$, $\lim_{\gamma\to+\infty} p_t = 0$, $\lim_{\varsigma_t\to 0} p_t = 1$ and $\lim_{\varsigma_t\to+\infty} p_t = 0$.

From (3) and (6), the cumulative distribution function $H_t(y_t\,|\mathfrak{F}_{t-1})$ of Y_t becomes

$$\begin{aligned} H_t(y_t\,|\mathfrak{F}_{t-1}) \;=\; & \mathbb{I}(y_t = 0)\left[1 - \left(\frac{1}{1+\gamma}\right)^{\varsigma_t}\right] \\ & + \mathbb{I}(y_t > 0)\left[1 - \left(\frac{1}{1+\gamma}\right)^{\varsigma_t}\left(1+\frac{y_t}{\alpha_t}\right)^{-\varsigma_t}\right] \end{aligned}, \quad \gamma > 0, \quad \varsigma_t > 0, \quad \alpha_t > 0. \tag{7}$$

The formula in (7) combines two models from EVT: the POT for the conditional cumulative distribution function of exceedances; and the power law for the conditional probability of an exceedance. The model is a dynamic censored regression, the dynamic Tobit being an example of (see Hahn and Kuersteiner (2010) and references therein): compared to the dynamic Tobit, we replace the distributional assumption imposed on the underlying continuous dependent variable with an approximation for the conditional distribution of positive exceedances dictated by EVT.

2.2 Time-Varying Parameters

We resort to the observation-driven approach and apply the score-based mechanism of Creal *et al.* (2012) and Harvey (2013). The law of motion for $\varsigma_t > 0$ is specified in terms of an autoregressive process in exponential form as (see Harvey (2013))

$$\ln \varsigma_t = \phi_0 + \phi_1 \ln \varsigma_{t-1} + \phi_2 u_{t-1} : \tag{8}$$

ϕ_0, ϕ_1 and ϕ_2 are scalar parameters; $\ln \varsigma_{t-1}$ introduces the autoregressive component; and the update u_{t-1} requires $\phi_2 \neq 0$ for identification purposes (unless ϕ_1 is *a priori* known to be zero) and it is discussed more into details below.

Unlike the tail index, the scale $\alpha_t > 0$ enters the conditional distribution function in (7) only when a positive exceedance occurs (i.e., when $y_t > 0$) and we do not observe it over the entire sample period $t = 1, \ldots, T$: this potentially complicates modelling the dynamics of α_t. At the same time, if volatility clustering is not accounted for, movements in the tail will be confounded with movements in the scale due to model misspecification (see Harvey (2013), pp. $198 - 203$). We generalize Chavez-Demoulin *et al.* (2005) and model $\alpha_t > 0$ in exponential form as

$$\ln \alpha_t = \varphi_0 + \varphi_1 \ln \varsigma_{t-1} + \varphi_2 u_{t-1}, \tag{9}$$

where φ_0, φ_1 and φ_2 are scalar parameters: in writing (9) we implicitly assume that the components that determine the dynamics in ς_t also drive the law of motion for α_t. The model in (9) is more general than what suggested in Chavez-Demoulin *et al.* (2005), who assume that the realized exceedance is the only driver of the scale parameter (i.e., $\varphi_1 = 0$ and $u_t = y_t$): the estimation results in Sections 3.2 and 4.1 show that the tail index provides valuable information for understanding the time-varying properties of the scale parameter; and u_t is more generally data-driven, as further discussed below. Unlike McNeil and Frey (2000) and Poon *et al.* (2004), we do not apply GARCH-type models to the data to account for volatility clustering and then fit a static POT model: this strategy assumes that extreme returns follow the same distribution as the rest of the returns (Engle and Manganelli (2004)).

The key component in the law of motion for ς_t in (8) is the updating mechanism u_t: this is known given $\mathfrak{F}_t$ under the observation-driven approach. We model u_t through the data-driven score-based mechanism of Creal *et al.* (2012) and Harvey (2013): this relates the innovation u_t to the score of the underlying likelihood function, which is a known quantity given $\mathfrak{F}_t$. Formally, from (7) let $h_t(Y_t|\mathfrak{F}_{t-1})$ be the density function of Y_t, namely

$$\begin{aligned} h_t\left(Y_t\left|\mathfrak{F}_{t-1}\right.\right) &= \mathbb{I}\left(Y_t=0\right)\left[1-\left(\frac{1}{1+\gamma}\right)^{\varsigma_t}\right] \\ &\quad +\mathbb{I}\left(Y_t>0\right)\left[\left(\frac{1}{1+\gamma}\right)^{\varsigma_t}\frac{\varsigma_t}{\alpha_t}\left(1+\frac{Y_t}{\alpha_t}\right)^{-\varsigma_t-1}\right], \quad \gamma>0, \quad \varsigma_t>0, \quad \alpha_t>0: \end{aligned} \tag{10}$$

according to the score-based mechanism, u_t is known given $\mathfrak{F}_t$ and defined as

$$u_t=-\left\{\mathrm{E}\left\{\frac{\partial^2\ln\left[h_t\left(Y_t\left|\mathfrak{F}_{t-1}\right.\right)\right]}{\left(\partial\ln\varsigma_t\right)^2}\left|\mathfrak{F}_{t-1}\right.\right\}\right\}^{-1}\frac{\partial\ln\left[h_t\left(y_t\left|\mathfrak{F}_{t-1}\right.\right)\right]}{\partial\ln\varsigma_t},$$

where (see Appendix A for details) the realized score with respect to $\ln\varsigma_t$ is

$$\begin{aligned} \frac{\partial\ln\left[h_t\left(y_t\left|\mathfrak{F}_{t-1}\right.\right)\right]}{\partial\ln\varsigma_t} &= \mathbb{I}\left(y_t>0\right)\left\{1+\ln\left[\left(\frac{1}{1+\gamma}\right)^{\varsigma_t}\left(1+\frac{y_t}{\alpha_t}\right)_+^{-\varsigma_t}\right]\right\} \\ &\quad -\mathbb{I}\left(y_t=0\right)\left[\frac{\left(\frac{1}{1+\gamma}\right)^{\varsigma_t}}{1-\left(\frac{1}{1+\gamma}\right)^{\varsigma_t}}\right]\ln\left[\left(\frac{1}{1+\gamma}\right)^{\varsigma_t}\right], \end{aligned} \tag{11}$$

and the formula for the information quantity $\mathrm{E}\left\{\frac{\partial^2\ln\left[h_t\left(Y_t\left|\mathfrak{F}_{t-1}\right.\right)\right]}{\left(\partial\ln\varsigma_t\right)^2}\left|\mathfrak{F}_{t-1}\right.\right\}$ is in Appendix A.

Notice that (8) and (9) jointly form a bivariate dynamic system with zero restrictions. There are several theoretical and empirical arguments supporting the dynamic score-based updating mechanism. Creal *et al.* (2012) point out that the score improves the local fit of the model in terms of likelihood contribution at time t given the value of the time-varying parameters at $t-1$: the score mechanism updates the parameters at time $t-1$ to more likely values at time t by taking the steepest ascent step in the direction of the score at $t-1$. The score therefore provides a natural updating mechanism, as it links the dynamics of the parameters to the likelihood of observing the realized data sample. Creal *et al.* (2012) further show that this new class of models nests a variety of popular specifications such as the GARCH (Bollerslev (1986)) and the ACD (Engle and Russell (1998)). Blasques *et al.* (2014) prove that the score method is information theoretic optimal, in the sense that the parameter updates always reduce the local Kullback-Leibler divergence between the true conditional density and the model implied conditional density. Harvey (2013) relates the dynamic score-based update to the unobserved components described in Harvey (1989): this makes the model we propose suitable to study the connections between tail risk and the macroeconomic environment; and it links our work to several contributions that advocate component models to look at volatility dynamics (see Engle *et al.* (2013) and references therein).

2.3 Estimation and Inference

2.3.1 Threshold Value

As in Quintos *et al.* (2001), Chavez-Demoulin and Embrechts (2004), and Chavez-Demoulin *et al.* (2014), we keep γ in (7) fixed over the entire sample and set it equal to a prespecified quantile of the empirical distribution of returns (see Section 2.1). The choice of γ creates a trade-off between model misspecification and estimation noise, which leads to a trade-off between bias and efficiency. A low γ makes many observations with $y_t > 0$ available to estimate the parameters of $H_t\left(y_t \,|\mathfrak{F}_{t-1}\right)$; at the same time, the GPD may provide a poor approximation to the true unknown underlying distribution. A high γ is consistent with the theoretical limiting result in (2); however, only few exceedances become available. The literature has proposed rigorous methods to select γ (see Scarrot and MacDonald (2012)). We follow Chavez-Demoulin and Embrechts (2004) and Chavez-Demoulin *et al.* (2014), and *a priori* set γ such that 10% of the realized returns are classified as exceedances: Chavez-Demoulin and Embrechts (2004) show that small variations in γ lead to little variation in parameter estimates. A line of future research would be to choose the threshold by extending to our dynamic setting the method Clauset *et al.* (2009) propose for a static framework: this requires minimizing above the threshold the distance between the actual distribution of the data and the one implied by the model.

2.3.2 Maximum Likelihood Estimation

Let $\boldsymbol{\theta} = (\phi_0, \phi_1, \phi_2, \varphi_0, \varphi_1, \varphi_2)'$ denote the vector of parameters that characterize the laws of motion for ς_t and α_t in (8) and (9), respectively: from the observation-driven approach, the conditional distribution of Y_t given the information set $\mathfrak{F}_{t-1}$ is known up to $\boldsymbol{\theta}$. Score-based models can be estimated by maximum likelihood (Creal *et al.* (2012) and Harvey (2013)): we then suitably extend the maximum likelihood estimator discussed in Smith (1985) and Davison and Smith (1990). From (7), the likelihood contribution from the realization $Y_t = y_t$ is

$$\begin{aligned} h_t\left(y_t \left|\mathfrak{F}_{t-1}\right.\right) &= \mathbb{I}\left(y_t = 0\right)\left[1 - \left(\frac{1}{1+\gamma}\right)^{\varsigma_t}\right] \\ &\quad + \mathbb{I}\left(y_t > 0\right)\left[\left(\frac{1}{1+\gamma}\right)^{\varsigma_t}\frac{\varsigma_t}{\alpha_t}\left(1 + \frac{y_t}{\alpha_t}\right)_+^{-\varsigma_t - 1}\right] \end{aligned}, \quad \gamma > 0, \quad \varsigma_t > 0, \quad \alpha_t > 0:$$

the maximum likelihood estimator $\hat{\boldsymbol{\theta}}$ for the true vector of parameters $\boldsymbol{\theta}^*$ solves $\hat{\boldsymbol{\theta}} = \arg\max_{\boldsymbol{\theta}} L\left(\boldsymbol{\theta}\right)$, where $L\left(\boldsymbol{\theta}\right) = \prod_{t=1}^{T} h_t\left(y_t \left|\mathfrak{F}_{t-1}\right.\right)$ is the likelihood function. In the static case, Smith (1985) provides sufficient conditions for the maximum likelihood estimator of the GPD to be consistent, asymptotically normally distributed and efficient. In the dynamic set up we consider, we proceed as in Creal *et al.* (2012) and conjecture that under appropriate regularity conditions $\hat{\boldsymbol{\theta}}$ is consistent and satisfies $T^{1/2}\left(\hat{\boldsymbol{\theta}} - \boldsymbol{\theta}^*\right) \xrightarrow{d} \mathcal{N}\left(\boldsymbol{0}, \boldsymbol{\Omega}^*\right)$, where $\boldsymbol{\Omega}^* = -\mathrm{E}\left[\left.\frac{\partial^2 \log L\left(\boldsymbol{\theta}\right)}{\partial\boldsymbol{\theta}\partial\boldsymbol{\theta}'}\right|_{\boldsymbol{\theta}=\boldsymbol{\theta}^*}\right]$.

3 Results from the U.S. Stock Market

3.1 Data

We use daily observations from the Center for Research in Security Prices (CRSP) and consider two sets of data: the value-weighted price index for NYSE, AMEX, and NASDAQ; and the price indices for size-sorted decile portfolios. From each index value, we construct the realized return r_t as the percentage continuously compounded return. The sample period begins in January

1954 and ends in December 2012, a total of 14851 daily observations: the long time series of available data allows to conduct inference on extreme returns, which we define by setting the threshold γ as discussed in Section 2.3.1. We gain information about market wide tail risk from the returns on the value-weighted portfolio. Decile-sorted portfolios let us study tail risk dynamics across different firm sizes: Decile 1 and Decile 10 portfolios correspond to the smallest (i.e., small caps) and the largest firms (i.e., large caps), respectively, and firm size monotonically increases from the former to the latter. Decile sorted portfolios allow us to interpret tail risk dynamics through the lens of Gabaix (2011) granular hypothesis of fluctuations.

Table 1 about here

Table 1 shows that returns from the value-weighted index and from the large caps portfolio have similar features. The portfolio mean decreases in market size, and the first four decile portfolios have lower standard deviation than the remaining six: the portfolios from the two sets of smaller firms are optimal in a mean-variance sense. All portfolio returns exhibit negative skewness and excess kurtosis: the null hypothesis of Gaussianity is always rejected.

3.2 Estimation Results

We perform the empirical analysis in Ox 7.1 (Doornik (2012)): the maximization algorithm is implemented with starting values ς_1 and α_1 equal to the estimates from the static model obtained by setting $\phi_1 = \phi_2 = 0$ and $\varphi_1 = \varphi_2 = 0$ in (8) and (9), respectively. Table 2 collects estimation results of the model in (7), (8) and (9) for negative and positive exceedances.

Table 2 about here

The results for negative exceedances (see Panel A) show that ϕ_1 is statistically significant at any conventional level: it is very close to unity, meaning that tail risk is highly persistent both at market level and across firm size, a result analogous to what found for returns volatility (see Andersen *et al.* (2003) and references therein); ϕ_1, and therefore the degree of persistence, is increasing in firm size. Analogous results apply to positive exceedances (see Panel B), where the persistence of the tail index is more pronounced than it is for negative exceedances. The parameter ϕ_2 is always greater than zero for both negative and positive exceedances: this resembles the empirical findings in the GARCH literature and strengthens the analogy between the two classes of models. Overall, the shape parameter displays rich dynamics across all firm sizes and along both tails of the conditional distribution of returns. The behavior of the scale parameter is asymmetric and linked to firm size. In the case of negative exceedances, the Wald statistic $\text{Wald}_{\varphi_1=\varphi_2=0}$ shows that the joint null hypothesis $\varphi_1 = \varphi_2 = 0$ is rejected only by Decile 10 and value-weighted portfolios: only large firms display statistically significant dynamics, which are then induced also on the market portfolio. As for positive exceedances, Deciles 1, 2 and 3 portfolios exhibit the strongest time-varying behavior.

Table 3 about here

We provide insights on the unconditional distribution of estimated daily tail indices in Table 3, where we report descriptive statistics for negative and positive exceedances, and correlations between the two for each equity portfolio. The sample period is $1955 - 2012$, a total of 14600 observations: we exclude estimates from 1954 to 1955 to minimize the effects induced by the starting values chosen in the estimation algorithm previously discussed. The descriptive statistics for negative exceedances (see Panel A) show that sample mean, standard deviation and median of ς_t all decrease with firm size: on average and median terms, tail risk is higher for larger firms than it is for smaller ones; and the volatility of tail risk decreases in firm size. The average value of the shape parameter exhibits substantial variation across firm size and falls between 3.549 (Decile 10) and 4.447 (Decile 2): these resemble values from studies that estimate static models using daily stock market returns and find that the tail index approximately ranges between 3 and 4.5 (Jansen and de Vries (1991) and Gabaix *et al.* (2003)). The empirical distribution of shape parameters is negatively skewed across all portfolios and the degree of skewness diminishes with firm size. Analogous qualitative results hold for positive exceedances (see Panel B). On the quantitative side, the average value of the shape parameter is higher for negative exceedances in the case of Deciles 1 to 4 and Decile 10, whereas it is higher for positive exceedances for Deciles 5 to 9; and the empirical distribution of the shape parameters is more negatively skewed in the case of negative exceedances across all portfolios. Finally, the correlation in daily shape parameters between negative and positive exceedances is positive and monotonically increasing in firm size (see Panel C).

Figure 1 plots the sequences of daily shape parameters estimated over the sample period $1955-2012$ for both negative and positive exceedances: to highlight the main features, we concentrate on value-weighted, small caps (i.e., Decile 1) and large caps (i.e., Decile 10) portfolios.

Figure 1 about here

Consistently with the results in Table 2, the sequence of tail indices for negative exceedances from large caps is more persistent than the one from small caps and it is similar to that from the value-weighted portfolio; it also shows a more pronounced cyclical behavior associated to stronger countercyclical tail risk. Analogous considerations hold for positive exceedances, where the series are more persistent than the counterparts from negative exceedances. The graphical analysis suggests that large firms tail risk may be related to the business cycle more than small firms tail risk: we provide stronger evidence of this in Section 3.3.

Figure 1 shows that the sequences of tail indices for small caps have upper bounds approximately equal to 5 and 4.75 for negative and positive exceedances, respectively. These bounds are understood through equation (11), which decomposes the score into two parts: one relates to exceedance observations and depends on the exceedance y_t, the tail index ς_t and the scale parameter α_t; the second pertains to non-exceedance observations and it is a function of the shape parameter ς_t only. Exceedance observations lead to higher variation in the sequence of tail indices than non-exceedance counterparts: the higher the number of consecutive exceedances, the more pronounced the variation in ς_t; conversely, ς_t becomes close to a constant value during periods of clustered non-exceedances. In our data, exceedances in small firms returns are more clustered than exceedances in large firms returns: the shape parameter for small firms displays a more pronounced tendency to remain close to a constant value, which puts a floor to the level of tail risk; by equation (11), convergence to this floor occurs because $u_t > 0$ when $y_t = 0$, which ensures a positive effect induced by the update on ς_t since the estimates of ϕ_2 are positive.

3.3 Links to the Macroeconomy

3.3.1 Non-Causal Analysis

Following Andersen *et al.* (2003), Kelly (2014) and Kelly and Jiang (2014), we treat the sequences of estimated shape parameters as the object of interest: this allows us to disregard estimation noise and the related econometric issues. We relate the sequences of shape parameters for negative and positive exceedances to key macroeconomic indicators tracking business cycle dynamics and macroeconomic uncertainty. We employ macroeconomic indicators at monthly frequency and aggregate daily sequences into monthly values by computing monthly medians: Kelly (2014) calculates averages within the month; unlike moments, quantiles are robust to outliers and the median is likely to provide more accurate information about the central tendency of the monthly distribution of tail indices (Kim and White (2004)); quantiles are also equivariant under monotone transformations and we can map monthly medians of tail indices into monthly medians of conditional probabilities of exceedances (see Section 3.3.3).

We consider several macroeconomic indicators. The first one is the recession dummy (RD), which takes unit value during recessions defined according to the NBER classification and it is otherwise equal to zero. Returns volatility is countercyclical (Schwert (1989)) and for each individual index we consider two measures of volatility: monthly realized volatility (RV), computed as the square root of the sum of squared daily returns within the month (Schwert (1989)); and the monthly long-run market volatility measure (LRV) proposed in Mele (2007). For each portfolio, we compute RV and LRV from the corresponding sequence of returns: this allows us to study the comovement between volatility and tail risk. Following Stock and Watson (2014), we consider five coincident indicators: industrial production (IP), nonfarm employment (EMP), real manufacturing and wholesale-retail trade sales (MT), real personal income less transfers (PIX) and the index published monthly by The Conference Board (TCB)[2]; we compute log-differences for IP (ΔIP), EMP (ΔEMP), MT (ΔMT), PIX (ΔPIX) and TCB (ΔTCB); other conditions being equal, an increase in ΔIP, ΔEMP, ΔMT, ΔPIX or ΔTCB signals an improvement in the underlying macroeconomic conditions. Finally, we analyze the linkages with macroeconomic uncertainty through the measures U(h) proposed in Jurado *et al.* (2015) for horizons $h = 1, 3, 12$: these are defined as the common variation in the unforecastable component of a large number of economic indicators[3]. The indicators RD, RV, LRV, U(1), U(3) and U(12) are countercyclical; ΔIP, ΔEMP, ΔMT, ΔPIX or ΔTCB are cyclical.

Table 4 about here

Table 4 collects results from correlation analysis, as suggested in Andersen *et al.* (2013) and in line with Kelly (2014). Due to data availability, correlations with macroeconomic indicators are computed using different sample periods: $1955:01-2012:12$ for RD, RV and LRV; $1960:01-2010:06$ for ΔIP, ΔEMP, ΔMT, ΔPIX and ΔTCB; and $1961:01-2011:11$ for U(1), U(3) and U(12). Starting from negative exceedances (see Panel A), tail risk is countercyclical.

[2] We thank Mark Watson for making the dataset available online at http://www.princeton.edu/~mwatson/publi.html .

[3] We thank Sydney Ludvigson for making the dataset available online at http://www.econ.nyu.edu/user/ludvigsons/jlndata.zip

Negative correlations arise across all portfolios with RD, the volatility measures RV and LRV, and the uncertainty measures U(1), U(3) and U(12): higher tail risk in equity markets is associated with recessionary periods, higher volatility and higher macroeconomic uncertainty. We observe positive correlations with ΔIP, ΔEMP, ΔMT, ΔPIX and ΔTCB: higher tail risk is associated with a deterioration of macroeconomic fundamentals. Over all investment portfolios, tail risk is most highly correlated with the volatility measures RV and LRV; it is also strongly correlated with the macroeconomic uncertainty measures proposed in Jurado *et al.* (2015). Similar results hold for positive exceedances (see Panel B).

As a final and most important result, Table 4 shows that the correlation between the sequences of tail indices and business cycle macroeconomic indicators (i.e., RD, ΔIP, ΔEMP, ΔMT, ΔPIX, ΔTCB, U(1), U(3) and U(12)) is monotonically stronger in firm size along both tails of the conditional distribution of returns. This is in line with the fact that the correlation in the shape parameters between negative and positive exceedances increases in firm size, as shown in Panel C of Table 3 (see Section 3.2). To the very best of our knowledge, the empirical fact we document is new to the literature and deserves further explanation. Since we estimate our model on stock returns, negative and positive tail estimates are informative about the growth rates distribution of the underlying firms: our tail risk estimates then proxy micro uncertainty in relation to firm size. We therefore relate to an important literature measuring micro uncertainty (see Bloom (2014)). At firm level, Bloom *et al.* (2014) document a significant increase in the interquartile range of sales growth and stock returns during contractionary periods: this is equivalent to saying that the percentiles of the cross-sectional distribution of sales growth and stock returns widen during recessions. The results in Bloom *et al.* (2014) relate to quantiles in both the left and the right hand-side of the conditional distribution of growth rates and stock returns: the distribution of growth rates at firm level then widens during recessions.

We differ from existing studies and contribute to the literature in the following way. We show that negative and positive tail risk of large firms increases more during recessions than tail risk of small firms: since we use a fixed threshold as discussed in Section 2.3.1, an equivalent interpretation is that the quantiles of the cross-sectional distribution of large firms widen during recessions more than the quantiles of the cross-sectional distribution of small firms; in other words, the distribution of large firms widens during recessions as compared to expansionary periods more than the distribution of small firms. Our findings differ from those in Bloom *et al.* (2014) in that we document that the dynamics of the cross-sectional distribution of firms over the business cycle depend on firm size: Bloom *et al.* (2014) show that firm-level uncertainty increases during recessions; we make one further step and show that uncertainty of large firms raises during recessions more than uncertainty of small firms.

3.3.2 Causal Analysis 1: Tail Risk and the Granular Hypothesis of Fluctuations

Table 4 shows that the correlation between tail indices and the business cycle increases in firm size (see discussion in Section 3.3.1): to the very best of our knowledge, this empirical fact has not been previously documented; it represents an important contribution of our paper and deserves further discussion. We argue that this finding is in line with Gabaix (2011) granular hypothesis of aggregate fluctuations: since the distribution of firms is highly fat-tailed, the central limit theorem does not apply and idiosyncratic shocks to large firms generate sizeable aggregate effects. Gabaix (2011) shows that idiosyncratic volatility of the largest 100 firms in the United States is responsible for approximately one-third of aggregate volatility. Carvalho and Gabaix (2013) argue that the granular volatility explains the Great Moderation and its undoing. The quantitative results in Carvalho and Grassi (2015) further support the granular hypothesis. We consider the potentially asymmetric effects of large firms negative and positive tail risk as opposed to those induced by volatility, which is a measure of symmetric dispersion. In order to link the non-causal results in Table 4 to the granular hypothesis, we run a causal analysis that tackles the following two issues.

Carvalho and Gabaix (2013) show that a granular economy with idiosyncratic shocks and demand linkages allows for a one factor representation that explains comovement in microeconomic-level variables. Under this common factor representation, large firms with a higher loading than small firms would be more sensitive to the common factor: compared to the granular hypothesis, the relationship of causality would be reversed. We assess the direction of causality between tail shocks to large firms and tail shocks to the economy through an identification strategy based on the time series (see Gabaix (2011), footnote 17) and resort to the notion of Granger causality: under the granular hypothesis, tail shocks to large firms Granger cause tail shocks to the economy, whereas the converse is not be true.

The second issue pertains to the causal impact on the economy of negative tail shocks in relation to positive tail shocks. The non-causal results in Table 4 show that large firms negative *and* positive tail risk increases during recessions. However, the granular hypothesis implies that only negative tail shocks lead recessionary periods. A testable implication then is that only negative tail shocks Granger cause tail shocks to the economy.

We consider usual mean regressions together with quantile regressions (Koenker and Bassett (1978)). The sample period is $1960:01-2010:06$. In the former case, we regress monthly median values of shape parameters for large caps (i.e., Decile 10 firms) for negative and positive exceedances on their lagged values and the lagged value of ΔIP: the models are informative about the causal effect of ΔIP (and therefore of the economy) on the tails of the distribution of large firms stock returns. We further construct regressions for the quantiles $\tau = 0.20, 0.80$ (see Giglio *et al.* (2015)) for the conditional distribution of ΔIP, with the same predictors as in the regressions against the mean: the models tell us whether tail shocks to large firms Granger cause tail shocks to the economy. The Granger causality analysis in Table 5 shows that ΔIP has no predictive power for tail risk on either side of the conditional distribution of large firms returns[4]. On the other hand, tail risk of large firms Granger causes the lower and upper tails

[4] Due to the high persistence in the dependent variable, the two equations for large caps have very high R^2: we run inference with respect to ΔIP and the resulting Granger causality remains valid (Sims et *al.* (1990)).

of the conditional distribution of ΔIP with the expected sign: a decrease in negative tail risk anticipates a rightward shift in the conditional distribution of ΔIP and then an improvement in the underlying conditions; and positive tail risk has no predictive power for the economy, a result in line with the literature (Allen *et al.* (2012) and Giglio *et al.* (2015)).

Table 5 about here

From our identification strategy we feel comfortable to safely conclude that Gabaix (2011) granular origin of fluctuations is consistent with the monotonic increase in firm size of the correlation between tail risk and the business cycle documented in Table 4. Tail risk Granger causes the underlying economy and the converse is not true. Further, only negative tail risk has predictive power for the economy: the positive correlation between positive tail risk and recessionary periods is due to the positive correlation between negative and positive tail risk documented in Panel C of Table 3, and it is not driven by any underlying causal effect.

3.3.3 Causal Analysis 2: Tail Risk, Micro Uncertainty and the Macroeconomy

We now run a second causal analysis and assess the macroeconomic impact of tail risk by estimating impulse response functions from a vector autoregressive (VAR) model similar to those constructed in Bloom (2009), Kelly and Jiang (2014) and Jurado *et al.* (2015). Our tail risk measures are informative about firm level shocks dispersion and therefore relate to micro uncertainty (Bloom (2014) and Bloom *et al.* (2014)): we then quantify the macroeconomic impact of micro uncertainty as measured by large firms tail risk.

We modify Kelly and Jiang (2014) VAR specification, which incorporates tail risk, to account for the granular hypothesis. The results in Table 5 show that large firms negative tail risk Granger causes large firms positive tail risk, whereas the converse is not true: we sequentially include large firms negative and positive monthly median tail probabilities, which are obtained from the underlying shape parameters through the equivariance property of quantiles; an increase in these probabilities denotes an increase in tail risk. Including large firms tail risk as the first elements of the VAR is consistent with the quantitative analysis in Carvalho and Grassi (2015): within their theoretical model, they look at the impact of negative shocks to the largest firm productivity on the economy[5]. We then add a measure of macro uncertainty to control for the aggregate economy: there now exist several measures of macro uncertainty (Bloom (2014)); we opt for monthly realized volatility from the value-weighted price index for NYSE, AMEX and NASDAQ, as it is comparable to our measures of tail risk (see Kelly and Jiang (2014), footnote 32). We finally include the Federal Funds Rate, log average hourly earnings, log consumer price index, hours, log employment and log industrial production[6]. We estimate the VAR over the period $1961:03 - 2011:12$ and select two lags as suggested by the BIC criterion.

Figure 2 about here

Figure 2 plots percentage changes in employment and industrial production induced by a one-standard deviation shock to negative and positive large firms tail risk, as well as percentage changes in the same variables due to a one-standard deviation shock to market realized volatility; the figure also reports 90% bootstrap coverage areas. A shock to negative tail risk induces a statistically significant reduction in employment, which reaches 0.2% after approximately 18 months, followed by a slow recovery; a shock to positive tail risk does not produce any statistically significant effect on employment. Similar results apply to industrial production: shocks to negative tail risk induce a reduction of 0.2% after approximately one year, whereas shocks to positive tail risk are not significant. These results are consistent with those in Table 5: negative tail risk leads the economy, whereas positive tail risk does not have any causal

[5] See Carvalho and Grassi (2015), Section 5.2.3.

[6] Average hourly earnings, hours and employment are calculated for the manufacturing sector as in Bloom (2009).

effect. Shocks to macro uncertainty, as measured by realized volatility, produce milder effects on employment and industrial production than shocks to negative tail risk. Shocks to tail risk then determine more extreme scenarios than shocks to volatility, which measures dispersion about the conditional mean: this is aligned with a strand of literature that stresses the importance of heavy-tailed shocks in asset pricing (see Gabaix (2012) and references therein); it implies that large firms negative tail risk shocks induce sizable effects on the economy.

As in Kelly and Jiang (2014), we find that shocks to negative tail risk have similar effects on employment and industrial production. We provide two additional contributions. We document the asymmetric response to shocks to negative and positive tail risk: this resembles previous results on the effects of systemic risk on the macroeconomy (Allen *et al.* (2012) and Giglio *et al.* (2015)). We quantify the impact of uncertainty shocks through the lens of Gabaix (2011) granular hypothesis by focusing on large firms only.

4 Evidence from International Stock Markets

4.1 Results

We use daily data from the MSCI indices and consider the G7 countries, namely Canada, France, Germany, Italy, Japan, the United Kingdom and the U.S.. We take the perspective of an unhedged U.S. investor and express all indices in U.S. dollars. From each index value, we construct the realized return r_t as the percentage continuously compounded return. The sample period begins in January 1975 and finishes in December 2012. We account for holidays by deleting observations from trading days for which at least one market has a return identically equal to zero: we end up with 9318 daily data points; and we define negative and positive exceedances as in Section 2.3.1. Table 6 shows that all returns exhibit negative skewness and excess kurtosis, and the null hypothesis of Gaussianity is always rejected at any conventional level; it also shows that the correlation between equity returns in G7 countries exhibits a great deal of variation, ranging between 0.059 (Japan and the U.S.) and 0.734 (France and Germany).

Table 6 about here

Table 7 about here

We collect estimation results in Table 7. The results for negative exceedances (see Panel A) show that ϕ_1 is statistically significant at any conventional level in all markets; it is very close to unity and falls between 0.981 (France) and 0.990 (Canada and the U.S.). Analogous results apply to positive exceedances (see Panel B): ϕ_1 ranges between 0.990 (France) and 0.996 (Canada). The parameter ϕ_2 is also positive across all markets and along both tails. Results from international markets confirm that tail risk is highly persistent over both sides of the conditional distribution of returns, and that persistency is more pronounced along the right tail. The shape parameter in international markets therefore displays analogous features as the tail index in the U.S. (see Table 2). The Wald statistic $\text{Wald}_{\varphi_1=\varphi_2=0}$ for the joint null hypothesis $\varphi_1 = \varphi_2 = 0$ shows that the dynamics in the scale parameter are more evident for negative than for positive exceedances. We provide further insights about the empirical distribution of the estimated sequences of shape parameters in Table 8.

Table 8 about here

The sample period is 1976−2012, a total of 9093 observations: we exclude estimates from 1975 to 1976 to minimize the effects induced by the starting values in the estimation algorithm discussed in Section 3. In the case of negative exceedances (see Panel A), the descriptive statistics show that the sample mean falls between 2.483 (Italy) and 3.228 (the U.S.) and that the empirical distribution is negatively skewed across all international portfolios; pairwise correlations are sizeable, ranging from 0.313 (Japan and the U.K.) to 0.757 (France and Germany). Analogous results hold for positive exceedances (see Panel B): exceptions are the empirical distributions for Germany, Japan and the United Kingdom, which are positively rather than negatively skewed.

4.2 Tail Connectedness

Given a set of risky assets, connectedness is measured with respect to the underlying metric and risk drivers: Kritzman *et al.* (2011) and Billio *et al.* (2012) apply principal components analysis to financial returns; Diebold and Yilmaz (2014) build several measures from variance decompositions to study realized volatilities. We build a measure of connectedness amongst the tails of the conditional distribution of returns: the tail index is a sufficient statistic for tail risk and we measure connectedness amongst the sequences of tail indices. We treat the estimated shape parameters as the direct object of interest (see Section 3.3). Let $\hat{\boldsymbol{\varsigma}}_t$ be the $N \times 1$ vector of estimated shape parameters from N portfolios of assets: we track the sequence $\{\hat{\boldsymbol{\varsigma}}_t\}_{t=1}^T$ and quantify connectedness using principal components as in Kritzman *et al.* (2011) and Billio *et al.* (2012). Let $\hat{\boldsymbol{\Sigma}} = T^{-1} \sum_{t=1}^T (\hat{\boldsymbol{\varsigma}}_t - \bar{\boldsymbol{\varsigma}}) (\hat{\boldsymbol{\varsigma}}_t - \bar{\boldsymbol{\varsigma}})'$ be the $N \times N$ sample covariance matrix of $\hat{\boldsymbol{\varsigma}}_t$, where $\bar{\boldsymbol{\varsigma}} = T^{-1} \sum_{t=1}^T \hat{\boldsymbol{\varsigma}}_t$ is the sample mean of $\hat{\boldsymbol{\varsigma}}_t$. Our measure of tail connectedness is the ratio between the maximum eigenvalue of $\hat{\boldsymbol{\Sigma}}$ and the sum of all eigenvalues of $\hat{\boldsymbol{\Sigma}}$: it lies within the unit interval by construction; it monotonically increases in connectedness among the elements of $\hat{\boldsymbol{\varsigma}}_t$, as the first principal component explains a higher portion of the variance of $\hat{\boldsymbol{\varsigma}}_t$. The measure quantifies the degree of cross-sectional dependence in tail risk amongst different assets.

International equity markets have different opening times and a synchronization issue arises. This does not pose any problem at the estimation stage in Section 4.1, as our model for tail risk is univariate. We now take a multivariate perspective and the synchronization problem has to be addressed. Poon *et al.* (2004) argue that the U.S. market drives all international markets; it is also the last one to close on any given day. Movements in the tails of U.S. returns are likely to drive movements in the tails of returns in international markets. We follow Poon *et al.* (2004) and use the previous day's U.S. tail index in building our measure of connectedness.

Figure 3 about here

Figure 3 plots tail connectedness measures estimated over 100−day rolling-sample windows for negative and positive exceedances. Both series exhibit cyclical behavior and high degree of time variation: the maximum eigenvalue explains between approximately 30% and almost 100% of the variation in tail risk; the two series have correlation equal to 0.489. The maximum eigenvalue captures most of the total variation during episodes of turmoil in financial markets such as: the 1987 stock market crash; the 1998 LTCM crisis; the dot-com bubble burst in early 2000s; the peak in 2005 followed by the Federal Reserve intervention that led to raised interest rates; and the recent financial crisis. Our results resemble those in Diebold and Yilmaz (2009) and suggest that diversification in global equity markets may not hedge against tail risk.

Finally, we uncover the drivers of global markets tail connectedness. We aggregate daily sequences by computing monthly medians of daily observations (see Section 3.3). We regress the resulting monthly series (expressed in percentage terms) of connectedness measures for negative and positive exceedances on a constant (CNT), the lagged values of both of them (CDN and CDP for negative and positive exceedances, respectively) and the lagged values of the following macroeconomic indicators: the average country-level realized volatility (VOL), which proxies global volatility (Gourio *et al.* (2013)); the G7 industrial production growth rate (GWT), measured as the percentage log-difference in seasonally adjusted industrial production; the G7 inflation rate (INF), measured as the percentage log-difference in CPI; and U.S. indicators, namely treasury bill rate (TBL), long-term yield (LTY), default yield spread (DFY) and unemployment rate (UNP). The sample period is 1976 − 2011, a total of 432 observations; the indicators are in line with those considered in Kelly (2014) and those tracked in the financial industry to measure macroeconomic risk.

Table 9 about here

Table 9 collects the results. Global tail connectedness has a strongly significant autoregressive component in both negative and positive exceedances. Volatility has a sizeable effect: joint extreme events are more likely to occur during periods of turmoil in financial markets (see Figure 3). Finally, negative exceedances connectedness Granger causes positive exceedances connectedness, whereas the converse is not true: this resembles the result in the mean regressions in Table 5 in relation to the causality between large firms negative and positive tail risk.

5 Concluding Remarks

This paper builds a novel dynamic peaks over threshold model with score-based time-varying parameters. We look at the linkages between tail risk and the macroeconomy: we show that large firms tail risk is more sensitive to the business cycle than small firms tail risk, which constitutes an original contribution to the literature on firm-level uncertainty (Bloom (2014) and Bloom *et al.* (2014)); we provide evidence that this finding is consistent with Gabaix (2011) granular hypothesis of aggregate fluctuations; we quantify the effect of large firms tail risk shocks on the economy. Finally, we introduce the concept of tail connectedness and show that in global equity markets tail connectedness increases during periods of turmoil.

A Updating Mechanism of Shape Parameter

Given the low of motion for ς_t in (8), let $\lambda_t = \ln \varsigma_t \Leftrightarrow \varsigma_t = \exp(\lambda_t)$: from (10), we have

$$\ln\left[h_t\left(y_t\left|\mathfrak{F}_{t-1}\right.\right)\right] = \mathbb{I}\left(y_t = 0\right)\ln\left[h_{0t}\left(y_t\left|\mathfrak{F}_{t-1}\right.\right)\right] + \mathbb{I}\left(y_t > 0\right)\ln\left[h_{1t}\left(y_t\left|\mathfrak{F}_{t-1}\right.\right)\right],$$

$$h_{0t}\left(y_t\left|\mathfrak{F}_{t-1}\right.\right) = 1 - \left(\frac{1}{1+\gamma}\right)^{\exp(\lambda_t)}, \qquad h_{1t}\left(y_t\left|\mathfrak{F}_{t-1}\right.\right) = \left(\frac{1}{1+\gamma}\right)^{\exp(\lambda_t)} \frac{\exp\left(\lambda_t\right)}{\alpha_t}\left(1+\frac{y_t}{\alpha_t}\right)^{-\exp(\lambda_t)-1}.$$

The score is

$$\frac{\partial \ln \left[h_t\left(y_t \left|\mathfrak{F}_{t-1}\right.\right)\right]}{\partial \lambda_t} = \mathbb{I}\left(y_t = 0\right) \frac{\partial \ln \left[h_{0t}\left(y_t \left|\mathfrak{F}_{t-1}\right.\right)\right]}{\partial \lambda_t} + \mathbb{I}\left(y_t > 0\right) \frac{\partial \ln \left[h_{1t}\left(y_t \left|\mathfrak{F}_{t-1}\right.\right)\right]}{\partial \lambda_t},$$

$$\frac{\partial \ln \left[h_{0t}\left(y_t \left|\mathfrak{F}_{t-1}\right.\right)\right]}{\partial \lambda_t} = -\frac{\left(\frac{1}{1+\gamma}\right)^{\exp(\lambda_t)}}{1-\left(\frac{1}{1+\gamma}\right)^{\exp(\lambda_t)}} \ln\left[\left(\frac{1}{1+\gamma}\right)^{\exp(\lambda_t)}\right],$$

$$\frac{\partial \ln \left[h_{1t}\left(y_t \left|\mathfrak{F}_{t-1}\right.\right)\right]}{\partial \lambda_t} = 1 + \ln\left[\left(\frac{1}{1+\gamma}\right)^{\exp(\lambda_t)}\left(1+\frac{y_t}{\alpha_t}\right)^{-\exp(\lambda_t)}\right],$$

and (11) follows. As for the information quantity,

$$\frac{\partial^2 \ln \left[h_t\left(Y_t \left|\mathfrak{F}_{t-1}\right.\right)\right]}{\partial \lambda_t^2} = \mathbb{I}\left(Y_t = 0\right) \frac{\partial^2 \ln \left[h_{0t}\left(Y_t \left|\mathfrak{F}_{t-1}\right.\right)\right]}{\partial \lambda_t^2} + \mathbb{I}\left(Y_t > 0\right) \frac{\partial^2 \ln \left[h_{1t}\left(Y_t \left|\mathfrak{F}_{t-1}\right.\right)\right]}{\partial \lambda_t^2},$$

$$\begin{aligned} \frac{\partial^2 \ln \left[h_{0t}\left(Y_t \left|\mathfrak{F}_{t-1}\right.\right)\right]}{\partial \lambda_t^2} &= -\left[\frac{\left(\frac{1}{1+\gamma}\right)^{\exp(\lambda_t)}}{1-\left(\frac{1}{1+\gamma}\right)^{\exp(\lambda_t)}}\right] \ln\left[\left(\frac{1}{1+\gamma}\right)^{\exp(\lambda_t)}\right] \\ &\quad \times \left\{1+\frac{1}{1-\left(\frac{1}{1+\gamma}\right)^{\exp(\lambda_t)}} \ln\left[\left(\frac{1}{1+\gamma}\right)^{\exp(\lambda_t)}\right]\right\}, \end{aligned}$$

$$\frac{\partial^2 \ln \left[h_{1t}\left(Y_t \left|\mathfrak{F}_{t-1}\right.\right)\right]}{\partial \lambda_t^2} = \ln\left[\left(\frac{1}{1+\gamma}\right)^{\exp(\lambda_t)}\left(1+\frac{Y_t}{\alpha_t}\right)^{-\exp(\lambda_t)}\right],$$

$$\begin{aligned} \frac{\partial^2 \ln \left[h_t\left(Y_t \left|\mathfrak{F}_{t-1}\right.\right)\right]}{\partial \lambda_t^2} &= \mathbb{I}\left(Y_t > 0\right)\left\{\ln\left[\left(\frac{1}{1+\gamma}\right)^{\exp(\lambda_t)}\left(1+\frac{Y_t}{\alpha_t}\right)^{-\exp(\lambda_t)}\right]\right\} \\ &\quad -\mathbb{I}\left(Y_t = 0\right)\left[\frac{\left(\frac{1}{1+\gamma}\right)^{\exp(\lambda_t)}}{1-\left(\frac{1}{1+\gamma}\right)^{\exp(\lambda_t)}}\right] \ln\left[\left(\frac{1}{1+\gamma}\right)^{\exp(\lambda_t)}\right] \\ &\quad \times \left\{1+\frac{1}{1-\left(\frac{1}{1+\gamma}\right)^{\exp(\lambda_t)}} \ln\left[\left(\frac{1}{1+\gamma}\right)^{\exp(\lambda_t)}\right]\right\}: \end{aligned}$$

this implies that

$$\begin{aligned} \mathrm{E}\left\{\frac{\partial^2 \ln\left[h_t\left(Y_t\left|\mathfrak{F}_{t-1}\right.\right)\right]}{\partial\lambda_t^2}\left|\mathfrak{F}_{t-1}\right.\right\} &= \mathrm{E}\left\{\mathbb{I}\left(Y_t>0\right)\left\{\ln\left[\left(\frac{1}{1+\gamma}\right)^{\exp(\lambda_t)}\left(1+\frac{Y_t}{\alpha_t}\right)^{-\exp(\lambda_t)}\right]\right\}\left|\mathfrak{F}_{t-1}\right.\right\} \\ &\quad -\left(\frac{1}{1+\gamma}\right)^{\exp(\lambda_t)}\ln\left[\left(\frac{1}{1+\gamma}\right)^{\exp(\lambda_t)}\right] \\ &\quad \times\left\{1+\frac{1}{1-\left(\frac{1}{1+\gamma}\right)^{\exp(\lambda_t)}}\ln\left[\left(\frac{1}{1+\gamma}\right)^{\exp(\lambda_t)}\right]\right\}. \end{aligned}$$

Notice that

$$\mathrm{E}\left\{\frac{\partial \ln\left[h_t\left(Y_t\left|\mathfrak{F}_{t-1}\right.\right)\right]}{\partial\lambda_t}\left|\mathfrak{F}_{t-1}\right.\right\}=0$$

$$\Leftrightarrow$$

$$\mathrm{E}\left\{\mathbb{I}\left(Y_t>0\right)\ln\left[\left(\frac{1}{1+\gamma}\right)^{\exp(\lambda_t)}\left(1+\frac{Y_t}{\alpha_t}\right)^{-\exp(\lambda_t)}\right]\left|\mathfrak{F}_{t-1}\right.\right\}=-\left(\frac{1}{1+\gamma}\right)^{\exp(\lambda_t)}\left\{1-\ln\left[\left(\frac{1}{1+\gamma}\right)^{\exp(\lambda_t)}\right]\right\}$$

and the following analytical expression for the information quantity is easily obtained

$$\mathrm{E}\left\{\frac{\partial^2 \ln\left[h_t\left(Y_t\left|\mathfrak{F}_{t-1}\right.\right)\right]}{\partial\lambda_t^2}\left|\mathfrak{F}_{t-1}\right.\right\}=-\left(\frac{1}{1+\gamma}\right)^{\exp(\lambda_t)}\left\{1+\frac{1}{1-\left(\frac{1}{1+\gamma}\right)^{\exp(\lambda_t)}}\left\{\ln\left[\left(\frac{1}{1+\gamma}\right)^{\exp(\lambda_t)}\right]\right\}^2\right\}.$$

References

[1] Akgiray, V. and G. G. Booth (1988), "The Stable-Law Model of Stock Returns," *Journal of Business and Economic Statistics*, 6 (1), 51 – 57.

[2] Allen, L. T. G. Bali and Y. Tang (2012), "Does Systemic Risk in the Financial Sector Predict Future Economic Downturns?" *Review of Financial Studies*, 25 (10), 3000 – 3036.

[3] Andersen, T. G., T. Bollerslev, P. F. Christoffersen and F. X. Diebold (2013), "Financial Risk Measurement for Financial Risk Management," in G. Constantinedes, M. Harris and Rene Stulz (eds.), *Handbook of the Economics of Finance, Volume 2, Part B*, Amsterdam, the Netherlands: Elsevier.

[4] Andersen, T.G., T. Bollerslev, F. X. Diebold and P. Labys (2003), "Modeling and Forecasting Realized Volatility," *Econometrica*, 71 (2), 579 – 625.

[5] Balkema, A. A. and L. De Haan (1974), "Residual Life Time at Great Age," *Annals of Probability*, 2 (5), 792 – 804.

[6] Billio, M., M. Getmansky, A. W. Lo and L. Pelizzon (2012), "Econometric Measures of Connectedness and Systemic Risk in the Finance and Insurance Sectors," *Journal of Financial Economics*, 104 (3), 535 – 559.

[7] Blasques, F., S. J. Koopman and A. Lucas (2014), "Information Theoretic Optimality of Observation Driven Time Series Models," Timbergen Institute Discussion Paper, *TI* $14 - 046/III$.

[8] Bloom, N. (2009), "The Impact of Uncertainty Shocks," *Econometrica*, 77 (3), 623 – 685.

[9] Bloom, N. (2014), "Fluctuations in Uncertainty," *Journal of Economic Perspectives*, 28 (2), 153 – 176.

[10] Bloom, N., M. Floetotto, N. Jaimovich, I. Saporta-Eksten and S. J. Terry (2014), "Really Uncertain Business Cycles," Working Papers 14 – 18, Center for Economic Studies, U.S. Census Bureau.

[11] Bollerslev, T. (1986), "Generalized Autoregressive Conditional Heteroskedasticity," *Journal of Econometrics*, 31 (3), 307 – 327.

[12] Bollerslev, T. (1987), "A Conditionally Heteroskedastic Time Series Model for Speculative Prices and Rates of Return," *Review of Economics and Statistics*, 69(3), 542 – 547.

[13] Carvalho, V. and X. Gabaix (2013), "The Great Diversification and its Undoing," *American Economic Review*, 105 (5), 1697 – 1727.

[14] Carvalho, V. and B. Grassi (2015), "Large Firm Dynamics and the Business Cycle," Working Paper, University of Cambridge and University of Oxford.

[15] Chavez-Demoulin, V. and A. C. Davison (2012), "Modelling Time Series Extremes," *Revstat - Statistical Journal*, 10 (1), 109 – 133.

[16] Chavez-Demoulin, V., A. C. Davison and A. J. McNeil (2005), "Estimating Value-at-Risk: A Point Process Approach," *Quantitative Finance*, 5 (2), 227 – 234.

[17] Chavez-Demoulin, V. and P. Embrechts (2004), "Smooth Extremal Models in Finance and Insurance," *Journal of Risk and Insurance*, 71 (2), 183 – 199.

[18] Chavez-Demoulin, V., P. Embrechts and S. Sardy (2014), "Extreme-Quantile Tracking for Financial Time Series," *Journal of Econometrics*, 188 (1), 44 – 52.

[19] Clauset, A., C. R. Shalizi and M. E. J. Newman (2009), "Power-Law Distributions in Empirical Data," *SIAM Review*, 51 (4), 661 – 703.

[20] Cox, D. R. (1981), "Statistical Analysis of Time Series: Some Recent Developments," *Scandinavian Journal of Statistics*, 8 (2), 93 – 115.

[21] Creal, D., S. J. Koopman and A. Lucas (2012), "Generalized Autoregressive Score Models with Applications", *Journal of Applied Econometrics*, 28 (5), 777 – 795.

[22] Davison, A. C. and R. L. Smith (1990), "Models for Exceedances over High Thresholds," *Journal of the Royal Statistical Society. Series B (Methodological)*, 52 (3), 393 – 442.

[23] Diebold, F. X., T. Schuermann, and J. D. Stroughair (1998), "Pitfalls and Opportunities in the Use of Extreme Value Theory in Risk Management," in A.-P. N. Refenes, A. N. Burgess and J. D. Moody (eds.), *Decision Technologies for Computational Finance*, Kluwer Academic Publishers.

[24] Diebold, F.X. and K. Yilmaz (2009), "Measuring Financial Asset Return and Volatility Spillovers, with Application to Global Equity Markets," *Economic Journal*, 119 (534), 158–171.

[25] Diebold, F.X. and K. Yilmaz (2014), "On the Network Topology of Variance Decompositions: Measuring the Connectedness of Financial Firms," *Journal of Econometrics*, 182 (1), 119 – 134.

[26] Doornik, J. A. (2012), *Ox 7: An Object-orientated Matrix Programming Language*, London: Timberlake Consultants Press.

[27] Embrechts, P., C. Klüppelberg and T. Mikosch (1997), *Modelling Extremal Events for Insurance and Finance*, Berlin: Springer-Verlag.

[28] Engle, R. F. (1982), "Autoregressive Conditional Heteroscedasticity with Estimates of the Variance of United Kingdom Inflation," *Econometrica*, 50 (4), 987 – 1007.

[29] Engle, R. F, E. Ghysels and B. Sohn (2013), "Stock Market Volatility and Macroeconomic Fundamentals," *Review of Economics and Statistics*, 95 (3), 776 – 797.

[30] Engle, R. F. and S. Manganelli (2004), "CAViaR: Conditional Autoregressive Value at Risk by Regression Quantiles," *Journal of Business and Economic Statistics*, 22 (4), 367 – 381.

[31] Engle R. F. and J. R. Russell (1998), "Autoregressive conditional duration: a new model for irregularly spaced transaction data," *Econometrica*, 66 (5), 1127 – 1162.

[32] Gabaix, X. (2011), "The Granular Origins of Aggregate Fluctuations," *Econometrica*, 79 (3), 733 – 772.

[33] Gabaix, X. (2012), "Variable Rare Disasters: An Exactly Solved Framework for Ten Puzzles in Macro-Finance," *Quarterly Journal of Economics*, 127 (2), 645 – 700.

[34] Gabaix, X., P. Gopikrishnan, V. Plerou and H. E. Stanley (2003), "A Theory of Power-Law Distributions in Financial Market Fluctuations," *Nature*, 423, 267 – 270.

[35] Galbraith, J. W. and S. Zernov (2004), "Circuit Breakers and the Tail Index of Equity Returns," *Journal of Financial Econometrics*, 2 (1), 109 – 129.

[36] Giglio, S., B. Kelly and S. Pruitt (2015), "Systemic Risk and the Macroeconomy: An Empirical Evaluation," *Journal of Financial Economics*, Forthcoming.

[37] Gourio, F., M. Siemer and A. Verdelhan (2013), "International Risk Cycles," *Journal of International Economics*, 89 (2), 471 – 484.

[38] Hahn, J. and G. Kuersteiner (2010), "Stationarity and mixing properties of the dynamic Tobit model," *Economics Letters*, 107 (2), 105 – 111.

[39] Hansen, B. E. (1994), "Autoregressive Conditional Density Estimation," *International Economic Review*, 35 (3), 705 – 730.

[40] Harvey, A. C. (1989), *Forecasting, Structural Time Series Models and the Kalman Filter*, Cambridge: Cambridge University Press.

[41] Harvey, A. C. (2013), *Dynamic Models for Volatility and Heavy Tails: With Applications to Financial and Economic Time Series*, Cambridge: Cambridge University Press.

[42] Hols, M. C. A. B. and C. G. de Vries (1991), "The Limiting Distribution of Extremal Exchange Rate Returns," *Journal of Applied Econometrics*, 6 (3), 287 – 302.

[43] Jansen, D. W. and C. G. de Vries (1991), "On the Frequency of Large Stock Returns: Putting Boom and Busts into Perspective," *Review of Economics and Statistics*, 73 (1), 18 – 24.

[44] Jurado, K., S. C. Ludvigson and S. Ng (2015), "Meauring Uncertainty," *American Economic Review*, 105 (3), 1177 – 1216.

[45] Kearns, P. and A. Pagan (1997), "Estimating the Density Tail Index for Financial Time Series," *Review of Economics and Statistics*, 79 (2), 171 – 175.

[46] Kelly, B. (2014), "The Dynamic Power Law Model," *Extremes*, forthcoming.

[47] Kelly, B. and H. Jiang (2014), "Tail Risk and Asset Prices," *Review of Financial Studies*, 27 (10), 2841 – 2871.

[48] Kim, T. and H. White (2004), "On More Robust Estimation of Skewness and Kurtosis," *Finance Research Letters*, 1 (1), 56 – 73.

[49] Koedijk, K.G., M. M. A. Schafgans and C. G. de Vries (1990), "The Tail Index of Exchange Rate Returns," *Journal of International Economics*, 29 (1 – 2), 93 – 108.

[50] Koenker, R. and G. Bassett (1978), "Regression Quantiles," *Econometrica*, 46 (1), 33 – 50.

[51] Kritzman, M., Y. Li , S. Page and R. Rigobon (2011), "Principal Components as a Measure of Systemic Risk," *Journal of Portfolio Management*, 37 (4), 112 – 126.

[52] Ledford, A. W. and J. A. Tawn (1996), "Statistics for Near Independence in Multivariate Extreme Values," *Biometrika*, 83 (1), 169 – 187.

[53] Longin, F. and B. Solnik (2001), "Extreme Correlation of International Equity Markets," *Journal of Finance*, 56 (2), 649 – 676.

[54] McNeil, A. J. and R. Frey (2000), "Estimation of Tail-Related Risk Measures for Heteroscedastic Financial Time Series: An Extreme Value Approach," *Journal of Empirical Finance*, 7 (3 – 4), 271 – 300.

[55] Mele, A. (2007), "Asymmetric Stock Market Volatility and the Cyclical Behavior of Expected Returns," *Journal of Financial Economics*, 86 (2), 446 – 478.

[56] Picklands, J. (1975), "Statistical Inference Using Extreme Order Statistics," *Annals of Statistics*, 3 (1), 119 – 131.

[57] Poon, S., M. Rockinger and J. Tawn (2004), "Extreme Value Dependence in Financial Markets," *Review of Financial Studies*, 17 (2), 581 – 610.

[58] Quintos, C., Z. Fan and P.C.B. Phillips (2001), "Structural Change Tests in Tail Behaviour and the Asian Crisis," *Review of Economic Studies*, 68 (3), 633 – 663.

[59] Scarrot, C. and A. MacDonald (2012), "A Review of Extreme Value Threshold Estimation and Uncertainty Quantification," *Revstat - Statistical Journal*, 10 (1), 33 – 60.

[60] Shephard, N. (2005), *Stochastic Volatility: Selected Readings*, Oxford: Oxford University Press.

[61] Schwert, G. W. (1989), "Why Does Stock Market Volatility Change Over Time?" *Journal of Finance*, 44 (5), 1115 – 1153.

[62] Sims, C. A., J. H. Stock and M. W. Watson (1990), "Inference in Linear Time Series Models with Some Unit Roots," *Econometrica*, 58 (1), 113 – 144.

[63] Smith, R. L. (1985), "Maximum Likelihood Estimation in a Class of Nonregular Cases," *Biometrika*, 72 (1), 67 – 90.

[64] Stock, J. H. and M. W. Watson (2014), "Estimating Turning Points Using Large Data Sets," *Journal of Econometrics*, 178 (2), 368 – 381.

[65] Wagner, N. (2005), "Autoregressive Conditional Tail Behavior and Results on Government Bond Yield Spreads," *International Review of Financial Analysis*, 14 (2), 247 – 261.

[66] Werner T. and C. Upper (2002), "Time Variation in the Behaviour of Bund Futures Returns," *Discussion Paper 25/02, Economic Research Centre of the Deutsche Bundesbank.*

Figure 1: Daily Shape Parameters, CRSP Portfolios, 1955-2012

This figure displays daily sequences of tail indices for negative and positive exceedances for Value-Weighted, Decile 1 (smallest firms) and Decile 10 (largest firms) portfolios. The sample period is $1955-2012$, a total of 14600 daily observations.

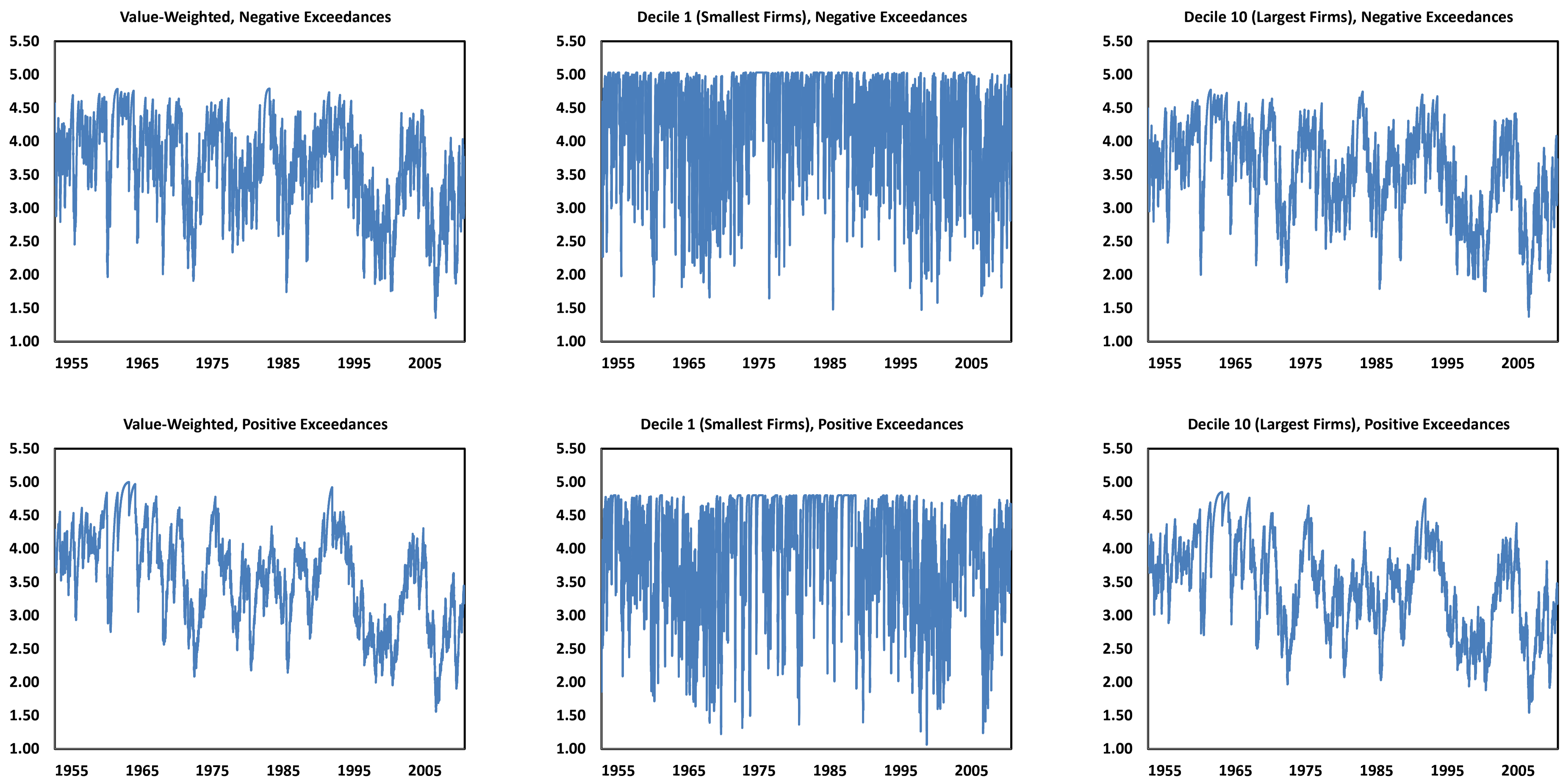

Figure 2: Tail Risk Impulse Response Functions, Large Firms CRSP Portfolio

This figure plots percentage changes in employment and industrial production induced by a one-standard-deviation shock to negative and positive large firms tail risk, as well as percentage changes in the same variables induced by a one-standard deviation shock to market realized volatility; the figure reports also 90% bootstrap coverage rates. In the underlying VAR specification, the following variables are sequentially included: large firms negative and positive tail risk, measured by monthly median values of exceedance probabilities; macro uncertainty, measured by monthly realized volatility from the value-weighted price index for NYSE, AMEX and NASDAQ; the Federal Funds Rate; log average hourly earnings; log consumer price index; hours; log employment; log industrial production.

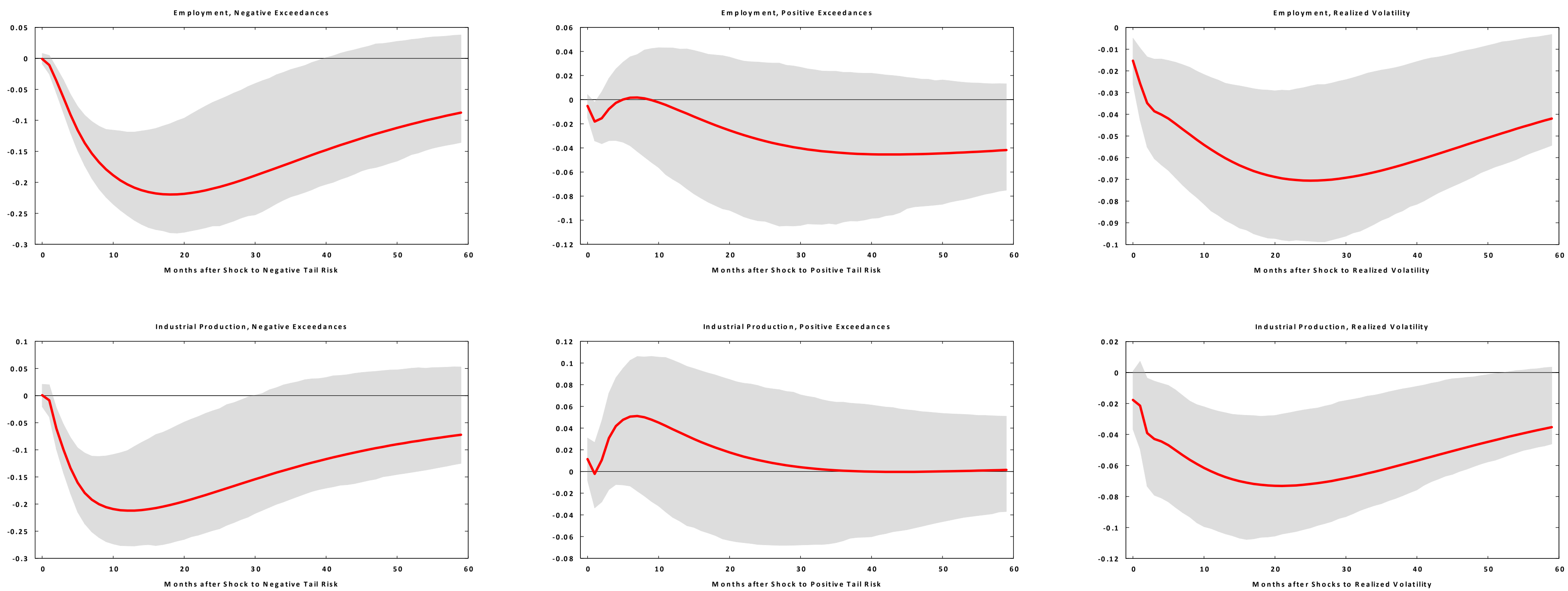

Figure 3: Daily Tail Connectedess Measures, International Portfolios, 1976-2012

This figure displays daily sequences of tail connectedness measures (in percentage terms) for negative and positive exceedances over the period 1976 − 2012, a total of 9093 daily observations. Estimation is carried out over a rolling window of 100 daily observations.

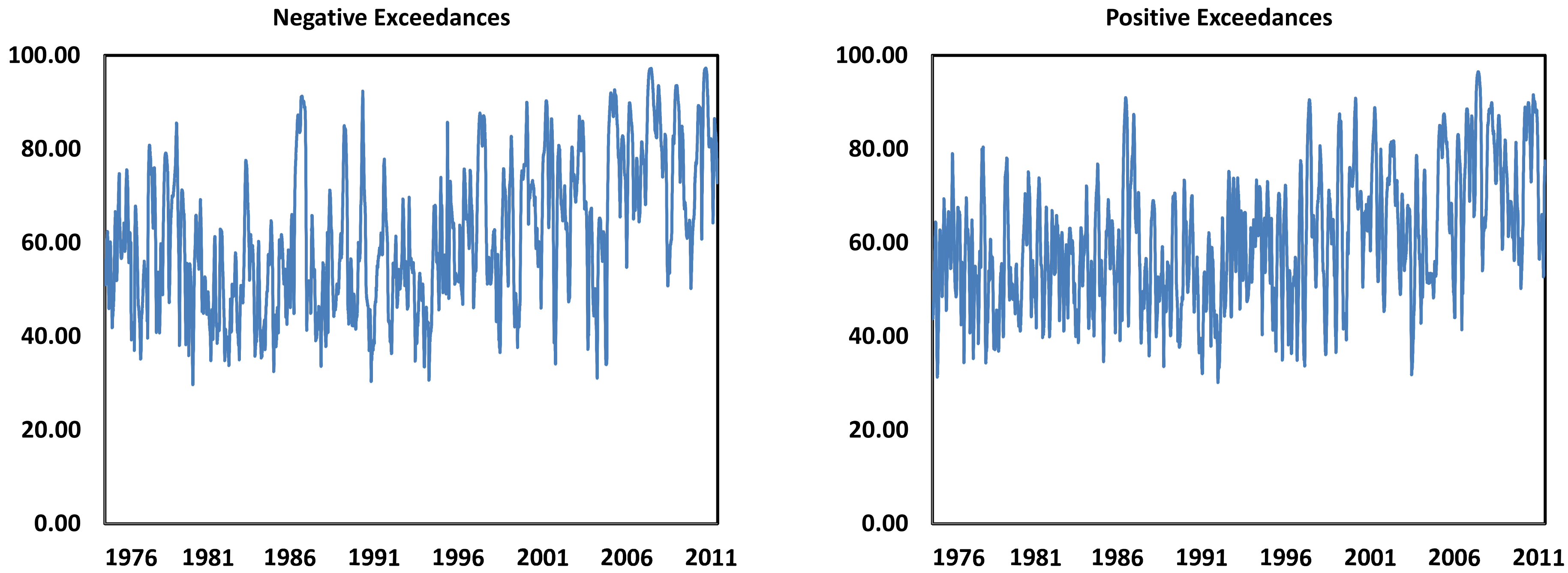

Table 1: Descriptive Statistics, Daily Returns, CRSP Portfolios, 1954-2012

This table presents descriptive statistics for the empirical distribution of daily returns from U.S. stock portfolios over the period $1954:01-2012:12$, a total of 14851 observations. Jarque-Bera denotes the Jarque-Bera goodness of fit test for normality: the joint null hypothesis is that skewness and kurtosis are equal to 0 and 3, respectively. *** indicates significance at the 1% level.

	Value-Weighted	Decile 1 (Smallest Firms)	Decile 2	Decile 3	Decile 4	Decile 5	Decile 6	Decile 7	Decile 8	Decile 9	Decile 10 (Largest Firms)
Mean	0.040	0.066	0.053	0.047	0.048	0.045	0.045	0.045	0.045	0.045	0.038
Std. Dev.	0.954	0.806	0.745	0.774	0.832	0.918	0.949	0.967	0.970	0.955	0.979
Median	0.074	0.089	0.089	0.098	0.104	0.102	0.108	0.105	0.105	0.098	0.063
Maximum	10.902	7.713	6.058	6.535	8.065	9.735	10.245	9.237	9.231	10.204	11.173
Minimum	-18.796	-8.535	-9.468	-11.151	-11.110	-12.150	-11.525	-12.202	-12.491	-14.214	-20.186
Skewness	-0.852	-0.356	-0.873	-1.153	-1.048	-0.949	-0.872	-0.825	-0.784	-0.836	-0.832
Kurtosis	22.848	12.219	13.544	16.429	15.734	17.531	16.570	15.438	16.244	17.527	24.357
Jarque-Bera ($\times 10^5$)	0.246***	0.529***	0.707***	1.149***	1.031***	1.329***	1.158***	0.974***	1.101***	1.323***	0.284***

Table 2: Estimation Results, Daily Returns, CRSP Portfolios, 1954-2012

This table reports estimation results for negative and positive exceedances. The sample period is $1954:01-2012:12$, a total of 14851 observations. Standard errors are in parentheses below parameter estimates. $\text{Wald}_{\varphi_1=\varphi_2=0}$ is the Wald test statistic for the null hypothesis $\varphi_1=\varphi_2=0$: the statistic is asymptotically distributed as χ^2 with 2 degrees of freedom. *, ** and *** indicate significance at the 10%, 5% and 1% levels, respectively. $^+$ indicates that the parameter ϕ_2 is *a priori* assumed to be different from 0.

Panel A: Negative Exceedances

	Value-Weighted	Decile 1 (Smallest Firms)	Decile 2	Decile 3	Decile 4	Decile 5	Decile 6	Decile 7	Decile 8	Decile 9	Decile 10 (Largest Firms)
Shape Parameter											
ϕ_0	0.017***	0.099***	0.126***	0.122***	0.092***	0.071***	0.050***	0.042***	0.036***	0.030***	0.013***
	(0.003)	(0.013)	(0.017)	(0.016)	(0.013)	(0.011)	(0.008)	(0.006)	(0.006)	(0.005)	(0.003)
ϕ_1	0.986***	0.930***	0.914***	0.915***	0.933***	0.946***	0.961***	0.967***	0.972***	0.977***	0.989***
	(0.003)	(0.009)	(0.011)	(0.011)	(0.009)	(0.008)	(0.006)	(0.005)	(0.004)	(0.004)	(0.002)
ϕ_2	0.032+	0.076+	0.085+	0.086+	0.075+	0.068+	0.057+	0.053+	0.049+	0.044+	0.027+
	(0.003)	(0.006)	(0.006)	(0.007)	(0.006)	(0.006)	(0.005)	(0.005)	(0.004)	(0.004)	(0.003)
Scale Parameter											
φ_0	0.833***	0.655***	0.455***	0.545***	0.530***	0.674***	0.605***	0.611***	0.710***	0.663***	0.950***
	(0.161)	(0.157)	(0.157)	(0.152)	(0.147)	(0.146)	(0.143)	(0.140)	(0.142)	(0.144)	(0.166)
φ_1	-0.366***	-0.184*	-0.006	-0.055	-0.038	-0.124	-0.081	-0.078	-0.162*	-0.124	-0.499***
	(0.136)	(0.116)	(0.113)	(0.112)	(0.115)	(0.119)	(0.120)	(0.119)	(0.120)	(0.120)	(0.142)
φ_2	-0.039**	-0.021	-0.015	0.002	-0.016	0.012	-0.010	-0.007	-0.008	-0.020	-0.037**
	(0.020)	(0.019)	(0.019)	(0.019)	(0.020)	(0.020)	(0.021)	(0.020)	(0.020)	(0.021)	(0.021)
$\text{Wald}_{\varphi_1=\varphi_2=0}$	9.753***	3.428	0.636	0.257	0.951	1.675	0.622	0.501	1.864	1.768	14.290***

Panel B: Positive Exceedances

	Value-Weighted	Decile 1 (Smallest Firms)	Decile 2	Decile 3	Decile 4	Decile 5	Decile 6	Decile 7	Decile 8	Decile 9	Decile 10 (Largest Firms)
Shape Parameter											
ϕ_0	0.007***	0.067***	0.066***	0.061***	0.032***	0.024***	0.017***	0.010***	0.012***	0.009***	0.007***
	(0.001)	(0.008)	(0.009)	(0.009)	(0.006)	(0.004)	(0.003)	(0.002)	(0.002)	(0.002)	(0.001)
ϕ_1	0.994***	0.950***	0.953***	0.957***	0.977***	0.982***	0.987***	0.992***	0.990***	0.993***	0.994***
	(0.001)	(0.006)	(0.006)	(0.006)	(0.004)	(0.003)	(0.002)	(0.002)	(0.002)	(0.002)	(0.001)
ϕ_2	0.019+	0.075+	0.073+	0.067+	0.047+	0.041+	0.034+	0.027+	0.029+	0.024+	0.020+
	(0.002)	(0.005)	(0.005)	(0.005)	(0.005)	(0.004)	(0.003)	(0.003)	(0.003)	(0.003)	(0.002)
Scale Parameter											
φ_0	0.425***	-0.487***	-0.729***	-0.492***	-0.083	-0.119	0.236**	0.281**	0.346***	0.487***	0.570***
	(0.163)	(0.111)	(0.115)	(0.125)	(0.134)	(0.130)	(0.138)	(0.133)	(0.137)	(0.146)	(0.168)
φ_1	-0.061	0.478***	0.650***	0.493***	0.186**	0.293***	0.028	0.003	-0.056	-0.174*	-0.212*
	(0.140)	(0.092)	(0.092)	(0.098)	(0.108)	(0.109)	(0.118)	(0.115)	(0.118)	(0.125)	(0.148)
φ_2	-0.029*	-0.039**	-0.013	-0.009	-0.018	0.014	0.008	-0.021*	-0.004	-0.029**	-0.038**
	(0.020)	(0.017)	(0.018)	(0.018)	(0.018)	(0.017)	(0.016)	(0.016)	(0.018)	(0.017)	(0.021)
$\text{Wald}_{\varphi_1=\varphi_2=0}$	2.199	34.465***	52.052***	26.575***	4.649*	7.347**	0.275	1.797	0.241	3.983	4.980*

Table 3: Descriptive Statistics and Correlations, Daily Shape Parameters, CRSP Portfolios, 1955-2012

This table reports descriptive statistics and summary correlations for the estimated sequence of daily shape parameters from U.S. stock portfolios over the period 1955 : 01 − 2012 : 12, a total of 14600 observations. *** indicates significance at the 1% level.

Panel A: Negative Exceedances											
	Value-Weighted	Decile 1 (Smallest Firms)	Decile 2	Decile 3	Decile 4	Decile 5	Decile 6	Decile 7	Decile 8	Decile 9	Decile 10 (Largest Firms)
Mean	3.623	4.266	4.447	4.265	4.043	3.801	3.661	3.618	3.654	3.732	3.549
Std. Dev.	0.699	0.762	0.782	0.761	0.733	0.699	0.687	0.704	0.721	0.748	0.688
Median	3.720	4.482	4.702	4.524	4.256	3.976	3.818	3.750	3.791	3.869	3.622
Maximum	4.793	5.034	5.193	4.982	4.789	4.560	4.479	4.486	4.581	4.753	4.775
Minimum	1.353	1.475	1.431	1.350	1.362	1.257	1.236	1.254	1.251	1.284	1.372
Skewness	-0.526	-1.016	-1.094	-1.069	-0.962	-0.890	-0.795	-0.701	-0.679	-0.635	-0.454
Kurtosis	2.612	3.237	3.444	3.324	3.078	2.976	2.833	2.675	2.636	2.635	2.517

Panel B: Positive Exceedances											
	Value-Weighted	Decile 1 (Smallest Firms)	Decile 2	Decile 3	Decile 4	Decile 5	Decile 6	Decile 7	Decile 8	Decile 9	Decile 10 (Largest Firms)
Mean	3.567	3.948	4.233	4.243	4.026	3.865	3.802	3.746	3.718	3.748	3.444
Std. Dev.	0.722	0.833	0.900	0.885	0.854	0.845	0.858	0.889	0.859	0.849	0.686
Median	3.641	4.177	4.460	4.464	4.197	3.983	3.918	3.856	3.843	3.855	3.487
Maximum	5.001	4.802	5.176	5.206	5.147	5.026	5.091	5.159	5.032	5.196	4.852
Minimum	1.557	1.062	1.174	1.335	1.509	1.297	1.325	1.349	1.304	1.393	1.541
Skewness	-0.207	-0.924	-0.866	-0.807	-0.630	-0.508	-0.393	-0.346	-0.375	-0.350	-0.128
Kurtosis	2.344	2.973	2.863	2.692	2.481	2.386	2.202	2.109	2.134	2.238	2.366

Panel C: Correlations between Positive Exceedances and Negative Exceedances											
Correlation	0.753***	0.187***	0.193***	0.280***	0.399***	0.477***	0.570***	0.622***	0.659***	0.678***	0.797***

Table 4: Correlations with Macroeconomic Indicators, Monthly Median Values of Daily Shape Parameters, CRSP Portfolios, 1955-2012

This table reports summary correlations between monthly medians of estimated daily tail indices and the following macroeconomic indicators: recession dummy (RD); monthly realized volatility (RV) and monthly long-run volatility (LRV); log-difference in industrial production (ΔIP), nonfarm employment (ΔEMP), real manufacturing and wholesale-retail trade sales (ΔMT), real personal income less transfers (ΔPIX) and the index published monthly by The Conference Board (ΔTCB); and macroeconomic uncertainty U(h) for horizons $h = 1, 3, 12$. Correlations with RD, RV and LRV are computed over the period $1955:01 - 2012:12$; correlations with ΔIP, ΔEMP, ΔMT, ΔPIX and ΔTCB are computed over the period $1960:01 - 2010:06$; correlations with U(1), U(3) and U(12) are computed over the period $1961:01 - 2011:11$. ** and *** indicate significance at the 5% and 1% levels, respectively.

Panel A: Negative Exceedances

	Value-Weighted	Decile 1 (Smallest Firms)	Decile 2	Decile 3	Decile 4	Decile 5	Decile 6	Decile 7	Decile 8	Decile 9	Decile 10 (Largest Firms)
RD	-0.355***	-0.160***	-0.231***	-0.227***	-0.256***	-0.271***	-0.264***	-0.270***	-0.267***	-0.289***	-0.371***
RV	-0.753***	-0.632***	-0.668***	-0.717***	-0.726***	-0.748***	-0.755***	-0.779***	-0.770***	-0.770***	-0.742***
LRV	-0.551***	-0.277***	-0.295***	-0.313***	-0.301***	-0.309***	-0.334***	-0.396***	-0.425***	-0.511***	-0.599***
ΔIP	0.273***	0.086**	0.108***	0.096**	0.159***	0.178***	0.195***	0.216***	0.219***	0.224***	0.278***
ΔEMP	0.411***	0.143***	0.157***	0.156***	0.232***	0.264***	0.299***	0.326***	0.347***	0.352***	0.427***
ΔMT	0.205***	0.082**	0.106***	0.112***	0.158***	0.167***	0.176***	0.188***	0.190***	0.191***	0.204***
ΔPIX	0.270***	0.104**	0.121***	0.122***	0.182***	0.202***	0.224***	0.241***	0.247***	0.251***	0.277***
ΔTCB	0.364***	0.120***	0.144***	0.147***	0.224***	0.249***	0.278***	0.302***	0.313***	0.319***	0.374***
U(1)	-0.488***	-0.133***	-0.259***	-0.275***	-0.341***	-0.374***	-0.367***	-0.393***	-0.411***	-0.436***	-0.507***
U(3)	-0.517***	-0.146***	-0.269***	-0.285***	-0.351***	-0.386***	-0.384***	-0.416***	-0.436***	-0.462***	-0.536***
U(12)	-0.519***	-0.099**	-0.209***	-0.222***	-0.298***	-0.337***	-0.346***	-0.391***	-0.423***	-0.453***	-0.546***

Panel B: Positive Exceedances

	Value-Weighted	Decile 1 (Smallest Firms)	Decile 2	Decile 3	Decile 4	Decile 5	Decile 6	Decile 7	Decile 8	Decile 9	Decile 10 (Largest Firms)
RD	-0.298***	-0.017	-0.110***	-0.139***	-0.204***	-0.220***	-0.239***	-0.263***	-0.261***	-0.277***	-0.309***
RV	-0.593***	-0.639***	-0.567***	-0.551***	-0.568***	-0.563***	-0.584***	-0.588***	-0.605***	-0.596***	-0.599***
LRV	-0.745***	-0.470***	-0.536***	-0.539***	-0.573***	-0.540***	-0.560***	-0.625***	-0.638***	-0.712***	-0.743***
ΔIP	0.277***	-0.003	0.048	0.095**	0.143***	0.202***	0.233***	0.248***	0.254***	0.261***	0.279***
ΔEMP	0.483***	0.131***	0.162***	0.203***	0.292***	0.352***	0.411***	0.449***	0.453***	0.466***	0.476***
ΔMT	0.146***	-0.042	-0.012	0.030	0.060	0.087**	0.110***	0.125***	0.119***	0.127***	0.150***
ΔPIX	0.276***	0.064	0.087**	0.125***	0.169***	0.186***	0.226***	0.239***	0.249***	0.250***	0.272***
ΔTCB	0.375***	0.049	0.093**	0.142***	0.212***	0.261***	0.309***	0.338***	0.342***	0.350***	0.374***
U(1)	-0.507***	-0.044	-0.208***	-0.273***	-0.382***	-0.418***	-0.435***	-0.462***	-0.460***	-0.479***	-0.507***
U(3)	-0.534***	-0.035	-0.197***	-0.266***	-0.373***	-0.415***	-0.441***	-0.473***	-0.475***	-0.499***	-0.535***
U(12)	-0.570***	0.029	-0.119***	-0.194***	-0.298***	-0.349***	-0.394***	-0.444***	-0.465***	-0.501***	-0.578***

Table 5: Granger Causality Analysis, 1960-2010

This table shows results from Granger causality analysis over the period $1960:01-2010:06$, a total of 606 observations. The mean regressions regress monthly median values of shape parameters for large caps (i.e., Decile 10 firms) for negative and positive exceedances on their lagged values and the lagged value of the log-difference for industrial production (ΔIP). The quantile regressions for the conditional distribution of ΔIP, for quantiles $\tau = 0.20, 0.80$, have the same predictors as the mean regressions. Robust standard errors are in parentheses below parameter estimates. *** indicates significance at the 1% level. $\bar{R}^2$ denotes the adjusted R^2.

	Mean Regressions		**Quantile Regressions**	
	Decile 10 (Largest Firms), Negative Exceedances	Decile 10 (Largest Firms), Positive Exceedances	ΔIP, $\tau = 0.20$	ΔIP, $\tau = 0.80$
CNT	0.321***	-0.024	-0.011***	-0.002
	(0.059)	(0.038)	(0.002)	(0.002)
ΔIP	0.356	0.796	0.334***	0.164***
	(1.595)	(0.989)	(0.038)	(0.039)
Decile 10 (Largest Firms), Negative Exceedances	0.900***	0.234***	0.003***	0.002***
	(0.033)	(0.029)	(0.001)	(0.001)
Decile 10 (Largest Firms), Positive Exceedances	0.009	0.765***	0.000	0.000
	(0.034)	(0.029)	(0.001)	(0.001)
$\bar{R}^2$	0.820	0.931	-	-

Table 6: Descriptive Statistics and Correlation Matrix, Daily Returns, International Portfolios, 1975-2012

This table presents descriptive statistics and correlation matrix for the empirical distribution of daily returns from international stock portfolios over the period 1975 : 01 – 2012 : 12, a total of 9318 observations. The countries are Canada (CAN), France (FRA), Germany (DEU), Italy (ITA), Japan (JPN), the United Kingdom (GBR) and the U.S. (USA). Jarque-Bera denotes the Jarque-Bera goodness of fit test for normality: the joint null hypothesis is that skewness and kurtosis are equal to 0 and 3, respectively. *** indicates significance at the 1% level.

Panel A: Descriptive Statistics							
	CAN	FRA	DEU	ITA	JPN	GBR	USA
Mean	0.024	0.028	0.025	0.013	0.024	0.033	0.031
Std. Dev.	1.192	1.414	1.427	1.567	1.356	1.328	1.114
Median	0.054	0.057	0.047	0.023	0.034	0.054	0.051
Maximum	10.278	11.849	11.594	12.470	12.272	12.161	11.043
Minimum	-14.245	-11.572	-13.739	-12.388	-18.300	-14.065	-22.827
Skewness	-0.799	-0.122	-0.204	-0.209	-0.097	-0.172	-1.128
Kurtosis	15.348	9.135	9.172	8.236	11.336	10.390	29.571
Jarque-Bera ($\times 10^5$)	0.602***	0.146***	0.149***	0.107***	0.270***	0.212***	2.761***

Panel B: Correlation Matrix							
	CAN	FRA	DEU	ITA	JPN	GBR	USA
CAN	1.000	0.473	0.461	0.380	0.182	0.471	0.653
FRA		1.000	0.734	0.608	0.257	0.648	0.379
DEU			1.000	0.596	0.271	0.596	0.386
ITA				1.000	0.204	0.511	0.291
JPN					1.000	0.249	0.059
GBR						1.000	0.366
USA							1.000

Table 7: Estimation Results, Daily Returns, International Portfolios, 1975-2012

This table reports estimation results for negative and positive exceedances from international portfolios. The sample period is 1975 : 01 − 2012 : 12, a total of 9318 observations. The countries are Canada (CAN), France (FRA), Germany (DEU), Italy (ITA), Japan (JPN), the United Kingdom (GBR) and the U.S. (USA). Standard errors are in parentheses below parameter estimates. $\text{Wald}_{\varphi_1=\varphi_2=0}$ is the Wald test statistic for the null hypothesis $\varphi_1 = \varphi_2 = 0$: the statistic is asymptotically distributed as χ^2 with 2 degrees of freedom. *, ** and *** indicate significance at the 10%, 5% and 1% levels, respectively. $^{+}$ indicates that the parameter ϕ_2 is *a priori* assumed to be different from 0.

Panel A: Negative Exceedances

	CAN	FRA	DEU	ITA	JPN	GBR	USA
Shape Parameter							
ϕ_0	0.011***	0.018***	0.013***	0.012***	0.014***	0.012***	0.011***
	(0.003)	(0.004)	(0.003)	(0.003)	(0.003)	(0.003)	(0.003)
ϕ_1	0.990***	0.981***	0.986***	0.987***	0.986***	0.988***	0.990***
	(0.003)	(0.004)	(0.003)	(0.004)	(0.004)	(0.003)	(0.003)
ϕ_2	0.027^{+}	0.034^{+}	0.031^{+}	0.029^{+}	0.030^{+}	0.029^{+}	0.024^{+}
	(0.004)	(0.004)	(0.004)	(0.004)	(0.004)	(0.003)	(0.003)
Scale Parameter							
φ_0	0.904***	0.951***	0.780***	0.669***	0.643***	0.543***	0.888***
	(0.187)	(0.197)	(0.173)	(0.174)	(0.196)	(0.188)	(0.207)
φ_1	-0.403**	-0.654***	-0.424**	-0.130	-0.280*	-0.225	-0.446**
	(0.177)	(0.220)	(0.195)	(0.208)	(0.216)	(0.203)	(0.192)
φ_2	-0.056**	-0.051**	-0.040	-0.080***	-0.065**	-0.067***	-0.020
	(0.024)	(0.030)	(0.032)	(0.033)	(0.035)	(0.026)	(0.032)
$\text{Wald}_{\varphi_1=\varphi_2=0}$	9.495***	11.172***	6.086**	6.340**	5.088*	7.178**	5.534*

Panel B: Positive Exceedances

	CAN	FRA	DEU	ITA	JPN	GBR	USA
Shape Parameter							
ϕ_0	0.004***	0.009***	0.005***	0.006***	0.008***	0.009***	0.006***
	(0.001)	(0.003)	(0.001)	(0.002)	(0.003)	(0.002)	(0.002)
ϕ_1	0.996***	0.990***	0.994***	0.994***	0.992***	0.991***	0.995***
	(0.001)	(0.003)	(0.001)	(0.002)	(0.003)	(0.002)	(0.002)
ϕ_2	0.019^{+}	0.023^{+}	0.019^{+}	0.020^{+}	0.020^{+}	0.025^{+}	0.017^{+}
	(0.002)	(0.003)	(0.003)	(0.003)	(0.003)	(0.003)	(0.002)
Scale Parameter							
φ_0	0.598***	0.675***	0.841***	0.736***	0.416**	0.413**	0.740***
	(0.175)	(0.214)	(0.200)	(0.193)	(0.228)	(0.192)	(0.224)
φ_1	-0.292**	-0.417**	-0.537***	-0.467**	-0.049	-0.197	-0.355**
	(0.171)	(0.241)	(0.228)	(0.236)	(0.257)	(0.210)	(0.210)
φ_2	-0.041**	-0.030	-0.010	-0.045**	-0.079***	-0.057**	-0.019
	(0.023)	(0.032)	(0.032)	(0.026)	(0.030)	(0.030)	(0.030)
$\text{Wald}_{\varphi_1=\varphi_2=0}$	5.348*	3.606	5.561*	6.158**	7.032**	4.157	3.127

Table 8: Descriptive Statistics and Correlation Matrix, Daily Shape Parameters, International Portfolios, 1976-2012

This table reports descriptive statistics and correlation matrix for the estimated sequence of daily shape parameters for negative and positive exceedances from international portfolios over the period $1976:01-2012:12$, a total of 9093 observations. The countries are Canada (CAN), France (FRA), Germany (DEU), Italy (ITA), Japan (JPN), the United Kingdom (GBR) and the U.S. (USA). *** indicates significance at the 1% level.

Panel A: Negative Exceedances

	Descriptive Statistics							Correlation Matrix							
	CAN	FRA	DEU	ITA	JPN	GBR	USA		CAN	FRA	DEU	ITA	JPN	GBR	USA
Mean	3.146	2.597	2.618	2.483	2.679	2.730	3.228	CAN	1.000***	0.620***	0.607***	0.472***	0.457***	0.567***	0.725***
Std. Dev.	0.629	0.428	0.484	0.426	0.473	0.479	0.595	FRA		1.000***	0.757***	0.695***	0.435***	0.731***	0.662***
Median	3.229	2.648	2.662	2.511	2.677	2.732	3.291	DEU			1.000***	0.615***	0.577***	0.588***	0.690***
Maximum	4.216	3.330	3.454	3.264	3.532	3.652	4.269	ITA				1.000***	0.332***	0.611***	0.479***
Minimum	1.242	1.241	1.204	1.173	1.328	1.179	1.343	JPN					1.000***	0.313***	0.518***
Skewness	-0.428	-0.503	-0.397	-0.379	-0.150	-0.175	-0.489	GBR						1.000***	0.597***
Kurtosis	2.324	2.678	2.562	2.513	2.188	2.575	2.599	USA							1.000***

Panel B: Positive Exceedances

	Descriptive Statistics							Correlation Matrix							
	CAN	FRA	DEU	ITA	JPN	GBR	USA		CAN	FRA	DEU	ITA	JPN	GBR	USA
Mean	3.164	2.563	2.614	2.419	2.558	2.722	3.138	CAN	1.000***	0.492***	0.532***	0.306***	0.361***	0.436***	0.716***
Std. Dev.	0.743	0.392	0.507	0.426	0.385	0.475	0.566	FRA		1.000***	0.695***	0.650***	0.418***	0.707***	0.591***
Median	3.124	2.592	2.601	2.416	2.547	2.688	3.168	DEU			1.000***	0.507***	0.586***	0.470***	0.676***
Maximum	4.623	3.366	3.725	3.346	3.444	3.706	4.3492	ITA				1.000***	0.276***	0.465***	0.396***
Minimum	1.395	1.516	1.485	1.335	1.499	1.467	1.552	JPN					1.000***	0.308***	0.507***
Skewness	-0.081	-0.325	0.178	-0.045	0.093	0.105	-0.161	GBR						1.000***	0.607***
Kurtosis	2.119	2.552	2.479	2.362	2.550	2.479	2.372	USA							1.000***

Table 9: Macroeconomic Determinants of Tail Connectedness, International Portfolios, 1976-2012

This table reports results from predictive regressions for monthly sequences of tail connectedness measures for negative and positive exceedances over the period $1976 - 2012$, a total of 432 observations. The predictors are a constant (CNT) and the lagged values of the following indicators: tail connectedness for negative and positive exceedances (CDN and CDP, respectively), average country-level realized volatility (VOL), G7 industrial production growth rate (GWT), G7 inflation rate (INF), treasury bill rate (TBL), long-term yield (LTY), default yield spread (DFY) and unemployment rate (UNP). Newey-West estimated standard errors are reported between parentheses below parameter estimates. *** indicates significance at the 1% level. $\bar{R}^2$ denotes the adjusted R^2.

	Negative Exceedances	Positive Exceedances
CNT	0.158^{***}	0.158^{***}
	(0.040)	(0.035)
CDN	0.700^{***}	0.175^{***}
	(0.033)	(0.045)
CDP	0.027	0.538^{***}
	(0.044)	(0.032)
VOL	0.010^{***}	0.006^{***}
	(0.002)	(0.002)
GWT	0.009	0.021
	(0.013)	(0.014)
INF	0.003	-0.023
	(0.041)	(0.048)
TBL	0.004	-0.006
	(0.005)	(0.004)
LTY	-0.009	0.004
	(0.006)	(0.005)
DFY	0.000	0.009
	(0.012)	(0.016)
UNP	0.000	-0.002
	(0.004)	(0.004)
$\bar{R}^2$	0.665	0.529